

Article

Assessment of Integrated Solutions for the Combined Energy Efficiency Improvement and Seismic Strengthening of Existing URM Buildings

Maria-Victoria Requena-Garcia-Cruz ^{1,*}, Julia Díaz-Borrego ², Emilio Romero-Sánchez ¹, Antonio Morales-Esteban ^{1,3} and Miguel-Angel Campano ²

¹ Department of Building Structures and Geotechnical Engineering, University of Seville, Av. Reina Mercedes, 2, 41012 Seville, Spain

² Department of Building Constructions I, University of Seville, Av. Reina Mercedes, 2, 41012 Seville, Spain

³ Institute of Architecture and Construction Sciences, University of Seville, Av. Reina Mercedes, 2, 41012 Seville, Spain

* Correspondence: mrequena1@us.es



Citation: Requena-Garcia-Cruz, M.-V.; Díaz-Borrego, J.; Romero-Sánchez, E.; Morales-Esteban, A.; Campano, M.-A. Assessment of Integrated Solutions for the Combined Energy Efficiency Improvement and Seismic Strengthening of Existing URM Buildings. *Buildings* **2022**, *12*, 1276. <https://doi.org/10.3390/buildings12081276>

Academic Editors: Anastasios Tsiavos, Ricardo Monteiro and Rita Bento

Received: 12 July 2022

Accepted: 16 August 2022

Published: 20 August 2022

Publisher's Note: MDPI stays neutral with regard to jurisdictional claims in published maps and institutional affiliations.



Copyright: © 2022 by the authors. Licensee MDPI, Basel, Switzerland. This article is an open access article distributed under the terms and conditions of the Creative Commons Attribution (CC BY) license (<https://creativecommons.org/licenses/by/4.0/>).

Abstract: The European building stock is an aging infrastructure, mainly built prior to building codes. Furthermore, 65% of these buildings are located in seismic regions, which need to be both energetic and seismically retrofitted to comply with performance targets. Given this, this manuscript presents integrated constructive solutions that combine both energy efficiency improvement and seismic strengthening. The goal and novelty is to design and to evaluate one-shot, compatible, noninvasive, and complementary solutions applied to the façades of buildings with a minimum cost. To do so, different constraints have been borne in mind: the urban environment, achievable seismic and energy performance targets, and reduced construction costs. The method was applied to an old Spanish neighbourhood constructed in the 1960s. Different retrofitting packages were proposed for an unreinforced masonry case study building. A sensitivity analysis was performed to assess the effects of each configuration. A benefit/cost ratio was proposed to comparatively assess and to rank the solutions. The results of the seismoenergetic performance assessment showed that improving the behaviour of walls leads to higher benefit ratios than improving the openings. However, this latter strategy generates much lower construction costs. Integrating seismic into energetic retrofitting solutions supposes negligible additional costs but can improve the seismic behaviour of buildings by up to 240%. The optimal solution was the addition of higher ratios of steel grids and intermediate profiles in openings while adding thermal insulation in walls and renovating the window frames with PVC and standard 4/6/4 double glazing.

Keywords: combined energy and seismic retrofit; building refurbishment; integrated interventions; energy saving; seismic retrofitting; unreinforced masonry walls

1. Introduction

1.1. Background and Motivation

Most existing buildings in the European Union (EU) are reaching their nominal life, resulting in a significant degradation of their structural and nonstructural elements as well as their constructive materials. Moreover, 80% of the European residential building stock was built prior to the implementation of restrictive standards [1]. Therefore, they have become obsolescent and do not comply with modern requirements in terms of seismic safety, energy efficiency, and living comfort [2]. This may result in the partial or total collapse of these obsolescent structures, considering that at least 40% of them are located in regions of moderate to high seismic hazard [3]. Furthermore, these buildings are characterised by a low energy performance since their energy consumption is up to 40% of the total energy consumed by the EU [4].

It is estimated that at least 65% of the EU building stock located in seismic regions needs to be both energetically and seismically retrofitted to comply with minimum acceptable targets [4]. Given this situation, the EU and national governments have shown a growing interest in the seismic strengthening and energy efficiency improvement of the building stock. In this context, the EU Green Deal was approved to achieve climate neutrality by 2050 [5]. To this end, the EU has established residential building retrofitting programmes to improve energy efficiency, focusing on reducing the risk of energy poverty. In addition, the new EU rules for energy consumption and emission management aim to improve energy efficiency by at least 32.5% by 2030 [5]. In the case of Spain, the national PRE5000 programme aims to promote energy refurbishment to ultimately reduce the energy consumption and the carbon emissions of the building stock. For this purpose, energy rehabilitation activities have been funded by the EU Next Generation Fund and in the framework of the Spanish Recovery, Transformation, and Resilience Plan.

Despite investing major economic resources for the reduction of energy consumption and pollution emissions, seismic safety has usually been omitted in retrofitting activities. Several agreements have been signed on seismic risk reduction, such as the Sendai Framework for Disaster Risk Reduction 2015–2030. This framework supports the application of science and technology to decision making in disaster risk reduction [6]. It also highlights the importance of novel analyses and methodologies in the seismic retrofitting of existing structures to improve earthquake safety and resilience. In this context, at the EU level, the Eurocode 8 (EC8) was proposed as a homogenisation tool to standardise seismic performance assessment and target behaviour [7].

Focusing on Spain, recent seismic events revealed the high seismic vulnerability of existing buildings, particularly after the 2011 Lorca earthquake. During this event, several buildings, especially unreinforced masonry (URM) structures, were damaged or collapsed, resulting in significant social and economic losses [8]. Spanish URM buildings present typical characteristics that make them highly vulnerable to earthquakes [9]: a lack of seismic design (they were built before the application of seismic regulations), mixed structures (URM walls and reinforced concrete (RC) frames), poor maintenance, degradation of materials due to ageing effects, a low quality of materials, and irregularities in floor plan and height. Past recent earthquakes in the EU have mainly impacted low-rise domestic masonry buildings, while more modern RC buildings, built following recent seismic regulations, have almost been unaffected [10]. Moreover, recent works on the damage accumulation on URM structures during seismic events pointed out that these structures show significant vulnerability to sequences of induced seismicity events [11]. A large number of these URM buildings can be found in Andalusia, which were mainly constructed in the 1960s–1970s. This region is located in southern Spain, and it is characterised by a moderate seismic hazard due to the convergence of the Eurasian–African tectonic plates. Hence, the seismic vulnerability of these buildings, coupled with the considerable seismic hazard, indicates their significant seismic risk.

These old buildings that can be usually found in Andalusia are also typified by a low energy performance. The large amount of energy needed to reach acceptable comfort conditions and the corresponding CO₂ emissions indicate the very scarce energy efficiency of these buildings [4]. In fact, in Spain, the energy consumption of residential buildings represents about 20% of the total consumption of the country, and this has been growing steadily over recent years [12]. This poor performance mainly stems from the lack of insulation of walls and roofs, poor performance of acclimatisation systems, and ineffective sun exposure. In addition, in Spain, 93% of residential buildings were built before the first national Energy Performance of Buildings Directive (EPBD), and only 0.3% of the existing residential buildings have been energetically rehabilitated [1].

1.2. Overview of Seismic and Energy Retrofitting Techniques

The circumstances described above highlight that the Spanish building stock needs a comprehensive retrofitting to achieve adequate requirements in terms of seismic and

energy target behaviours. URM building seismic retrofitting is based on four main strategies [13]: (a) reinforcing wall–wall and wall–slab connections, (b) increasing the rigidity of slabs, (c) improving the out-of-plane behaviour by adding tie rods or ring beams, and (d) strengthening masonry walls. The URM buildings built in the 1960s–1970s in Andalusia usually present rigid floors, ring beams, and good connections between walls and slabs. Therefore, techniques focused on improving the strength of masonry walls are the most effective. Within this strategy, the most implemented materials for the reinforcement of masonry panels are steel, used in profiles or grids, and fibre-reinforced polymers (FRPs), combined with mortar layers [13]. There are some other in-plane retrofitting techniques based on the implementation of a mortar joint technique. In [14], a collar-jointed wall was assessed to strengthen single-lead walls. However, the construction costs of these solutions are higher than the addition of steel grids or FRP strips.

Steel grids added to masonry walls are one of the most conventional retrofitting techniques [15]. They are usually combined with the shotcrete technique to add mortar layers as experimentally analysed and validated in [16]. In [17], an innovative system constituted by a pretensioned stainless-steel grid was tested. A full-scale masonry wall reinforced was subjected to nonlinear static (NLS) analyses. It was concluded that this solution could considerably increase the strength and ductility of the wall. In [18], cyclic tests on masonry walls reinforced with single- and double-layered steel grout were performed. The specimens could withstand larger imposed loads and displacements, proving the efficiency of the strengthening technique. Steel is also added as profiles to create structural window frame systems to improve the in-plane behaviour of the masonry building. In [19], this solution was added to stiffen the openings, and it was validated through a series of experimental tests. In [13], this system was numerically assessed and applied to a case study building, being the most effective solution compared with the addition of steel grids.

FRP combined with mortar layers was proved to enhance the strength of panels and to prevent from the diagonal shear failure of walls. In [20], the effectiveness of the FRP layout was parametrically and numerically analysed to improve the global seismic resistance of a URM specimen. In [21], the flexural and shear strengthening of URM panels through FRP bars was experimentally assessed. These works on the addition of FRP strips indicate that this material presents an extremely high strength/weight ratio, a high corrosion resistance, and easy application. However, it has a high economic cost. As an alternative to FRP strips, in [3], a novel composite material called textile-reinforced mortar (TRM) was experimentally validated. This consists of textile fibre reinforcement combined with inorganic matrices. It was concluded that it could produce a similar percentage of enhancement to FRP if the textile strips are carefully assessed.

Regarding energy performance, the most influential factor in the energy consumption of residential buildings is the energy invested in climate control (heating and cooling). This represents 47.8% of the total annual energy consumption in Spanish households [4]. Focusing on the old URM buildings in Andalusia, these are characterised by the generalised low economic level of the population. This means that these dwellings do not present integrated air-conditioning systems. Instead, they generally rely on inefficient systems whose energy consumption/comfort ratio benefit is not optimal. Therefore, controlling the energy demand resulting from the transfer through the envelope is the most effective measure to reduce the thermal consumption associated with residential climate control [12].

As concluded in [1], the main strategies to reduce the demand are increasing the thermal insulation in façades and the renovation of windows and/or glazing systems. The authors reached this conclusion after performing a bibliographic review of the energy rehabilitation measures developed for the Spanish housing stock. The increase in roof insulation is the third most used technique, while the implementation of solar shading is the fourth. In [22], the authors observed that indoor thermal conditions were substantially improved by increasing the façades' thermal properties, which led to a positive effect on the occupants' living comfort. In [12], different strategies were proposed for the enhancement of the behaviour of openings by: replacing the glazing (single, double, and low

emissivity) and frames (with or without thermal breaks). The authors concluded that the implementation of a 4-6-4 glazing without thermal breaks alone reduces the total energy demand of the building by 10%. In [23], the authors analysed the impact of energy efficiency measures in relation to the hydrothermal behaviour derived from the transfer of the external environment to the interior through the envelope. They pointed out the danger of moisture-related problems (risk of condensation, structural degradation, microbial growth) arising from an improper retrofitting of buildings, which can lead to the airtightness of the envelope. However, in general, the addition of thermal insulation on the back of façades reduces the risk of thermal bridges and condensation, presenting itself as an easier and safer solution [22].

The building's thermal and lighting performances, as well as its energy consumption, are affected by the energy exchange processes that take place between the envelope and its surrounding environment [24]. As demonstrated in [25], the urban background is one of the factors that most affect the final energy performance of the building. In fact, this can affect the energy consumption by up to $\pm 10\%$. Similarly, in [26], it was found that the building performance depends, to a large extent, on its position with regard to its urban surrounding. The authors pointed out that the urban environment has a direct effect on the building's air-conditioning loads. Therefore, the surrounding urban configuration must be taken into account to obtain the true potential energy saving that can be achieved [27]. In detailed analyses, different orientations of façades and energy saving analyses per dwelling will result in optimised actions in terms of material, environmental, and economic savings compared with single and uniform envelope solutions [12].

1.3. Combined Seismic and Energy Retrofitting Techniques

Until the last decade, seismic and energy retrofitting techniques were considered objectives to be achieved separately [28]. In some cases, the solutions were implemented without considering the benefits of performing integrated interventions. In [29], it was concluded that structural components had a larger impact on the economic losses than the energy performance if the structure was located in an earthquake-prone area. Additionally, it was pointed out that the energy retrofitting could affect the masses and structural configuration of the building, leading to a different seismic behaviour. In [28], different retrofitting techniques were assessed individually and then combined but not integrated. The solutions were classified according to the Italian seismic risk assessment. In [30], two different solutions were assessed to determine the benefits of the Italian tax incentives. The solutions were based on strengthening with reinforced plaster and the addition of thermal insulation of some structural walls selected randomly. It was concluded that tax incentives are essential to the profitability of building refurbishment [31]. In [32], a method was proposed to define fragility curves for RC buildings considering both the energy and the structural behaviour. Additionally, for RC buildings, in [33,34], a framework for the sustainable renovation of this type of buildings was proposed, comparing different solutions.

In some other cases, new systems that combine both performances were proposed. In fact, in [35], the authors discussed the benefits of proposing integrated approaches for the buildings' retrofitting from the thermal and structural point of view. It was concluded that composite materials can improve each performance while respecting the architectural requirements. Nevertheless, they are subjected to a proper experimental validation. In [36], a system composed of vertical steel profiles combined with thermal insulation was proposed. The equivalent frame (EF) method was followed to model the masonry panels, and diagonal trusses were added to account for the additional strength of the steel profiles. NLS analyses were performed to conclude that the ductility of the structure could be improved. However, there was not a specific analysis of the energy performance of the building or of the advantages of the system. In [3], an innovative technique that combined TRM-based composites with thermal insulation was numerically assessed. It was concluded that

the solution could be efficient to improve the seismic and energy performance but also financially feasible.

1.4. Scope and Novelty of the Work

Studies on the combined seismic strengthening and energy efficiency are very limited. A lack of clear strategies for the selection and analysis of integrated interventions to maximise the benefits is found. As suggested in several works, research on how the seismic and energy retrofitting systems can be combined in an integrated retrofitting solution is needed [37]. Furthermore, the sustainable retrofitting of existing buildings is a prerequisite for achieving climatic and energy objectives in the EU. Thus, practical tools supporting the evaluation and decision-making process when planning retrofit interventions are required [38].

Given this context, this work deals with the assessment of integrated seismic and energy retrofit techniques that are to be implemented in existing URM buildings. The novelty herein proposed consists in the design of one-shot, compatible, noninvasive, and complementary solutions applied to the façades of existing buildings. The goal is to assess solutions with a minimum cost, taking into account the urban environment while considering the following constraints: achievable structural and energy performance targets (i.e., using proper performance parameters or minimum targets prescribed by legislation), physical compatibility among techniques, disruption time, and harmonisation within the seismic and building codes in force. A benefit/cost ratio is used to comparatively assess and to rank the different seismic retrofitting techniques proposed [39]. The combination of the interventions is applied to an existing URM building selected as a case study building. This belongs to a typical neighbourhood constructed with the Mediterranean construction standard in the 1960s, and it is representative of the Andalusian residential building stock. The overall methodology allows the achievement of benefits from several points of view: cost-effectiveness solutions in the light of the construction costs and the reduction of the embodied energy (and corresponding CO₂ emissions) and the seismic damage, designed considering a minimum architectural impact, and the optimisation of resources during their implementation. The method followed in this research is shown in Figure 1. The definition of the variables shown in the flowchart is presented in Section 4.5.

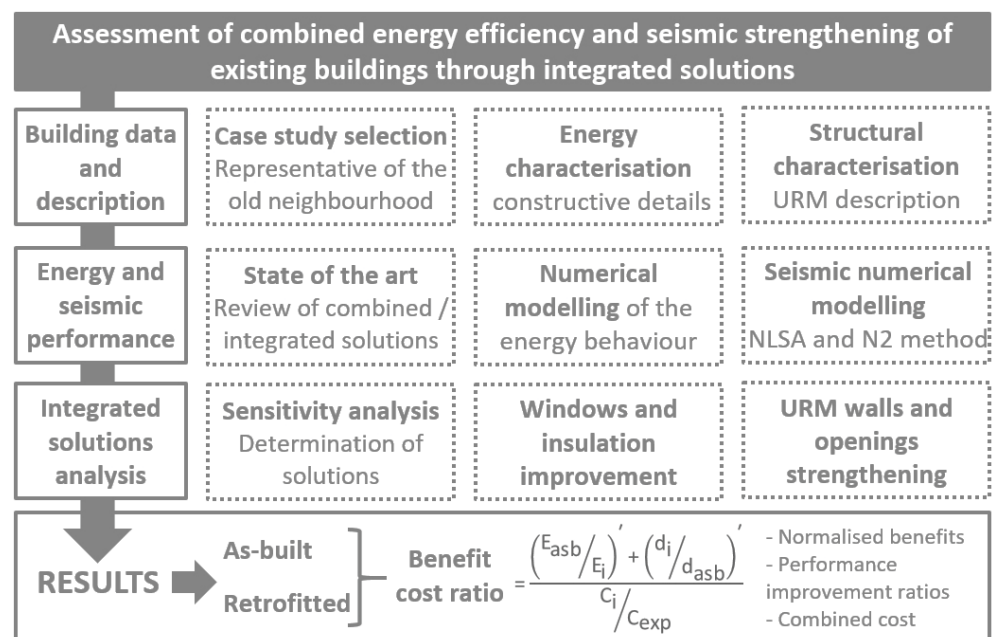


Figure 1. Flowchart of the work.

2. Case Study

2.1. 'El Plantinar' Neighbourhood

The old neighbourhood of 'El Plantinar' is located in Seville (Spain) (Figure 2), and it was constructed during the 1960s. It has been selected as case study since it is representative of the most widespread archetype old URM neighbours in Andalusia. The set is composed of three different types of buildings combined or separated by structural joints. They share the same structural configuration, URM walls in the perimeter and an interior RC frame. Despite being of five-storey height, the buildings present different structural distributions in plan and area. They were constructed before the application of energy and seismic codes in Spain. Therefore, they do not comply with energy behaviour targets, and they were built only considering gravitational loads (note that the first restrictive seismic code in force dates from 1994).



Figure 2. Case study neighbourhood and building location.

2.2. Case Study Building

In this work, the Type 1 building was selected to be analysed. It is the largest one, and it can be found isolated. This enables avoiding in the seismic analyses the possible effects of pounding between adjacent buildings [40]. This case study building is analysed in four different orientations, covering the different cases of urban location that can be found in the neighbourhood.

2.2.1. Structural Characterisation

The structural system of the building is based on RC ribbed slabs supported by external URM walls and an interior RC frame. URM walls were built with hollow ceramic bricks of $24\text{ cm} \times 11.5\text{ cm} \times 5\text{ cm}$. Their thickness varies according to height: at the ground floor, they are of 0.34 m, and at the rest of floors, 0.28 m. The ribbed slabs were built with prestressed concrete joists, ceramic vaults, a superficial concrete layer, and a narrow RC ring beam. According to its structural configuration, the rigid behaviour of slabs and the horizontal connections (to prevent the structure from out-of-plane failure) is guaranteed. In Table 1, the mechanical parameters are listed, which have been defined according to the blueprints and the mandatory construction code during that period, the Spanish MV-201 [41]. The distribution in plan considering the structural system and the elevation of the building is shown in Figure 3, including some photos taken by the authors. The gravitational loads were computed as in [42]. In total, the dead loads were 5.5 kPa, and the live loads 2 kPa (as suggested in the Spanish seismic code for residential buildings).

Table 1. Mechanical parameters.

| | | | | | | |
|----------------|--------------------------------|--------------------------|-----------------------------|------------------------|-------------------------|-----------------------------|
| Masonry | $\gamma = 18 \text{ kN/m}^3$ | $f_c = 4.0 \text{ MPa}$ | $f_{ck} = 1.14 \text{ MPa}$ | $E = 1200 \text{ MPa}$ | $G = 150 \text{ GPa}$ | $\tau_0 = 0.05 \text{ MPa}$ |
| RC | $\gamma = 25 \text{ kN/m}^3$ | $f_c = 25.5 \text{ MPa}$ | $f_{ck} = 17.5 \text{ MPa}$ | $E = 3000 \text{ GPa}$ | $G = 17000 \text{ GPa}$ | |
| Steel | $\gamma = 78.6 \text{ kN/m}^3$ | $f_y = 428 \text{ MPa}$ | $f_{yk} = 400 \text{ MPa}$ | $E = 210 \text{ GPa}$ | $G = 800 \text{ GPa}$ | |

γ is the specific weight, f_c is the compressive strength, f_{ck} is the characteristic compressive strength, τ_0 is the diagonal cracking strength of the masonry, E and G are the elastic and shear moduli, f_y is the yielding strength of rebar steel, and f_{yk} is the characteristic yielding strength of the rebar steel.

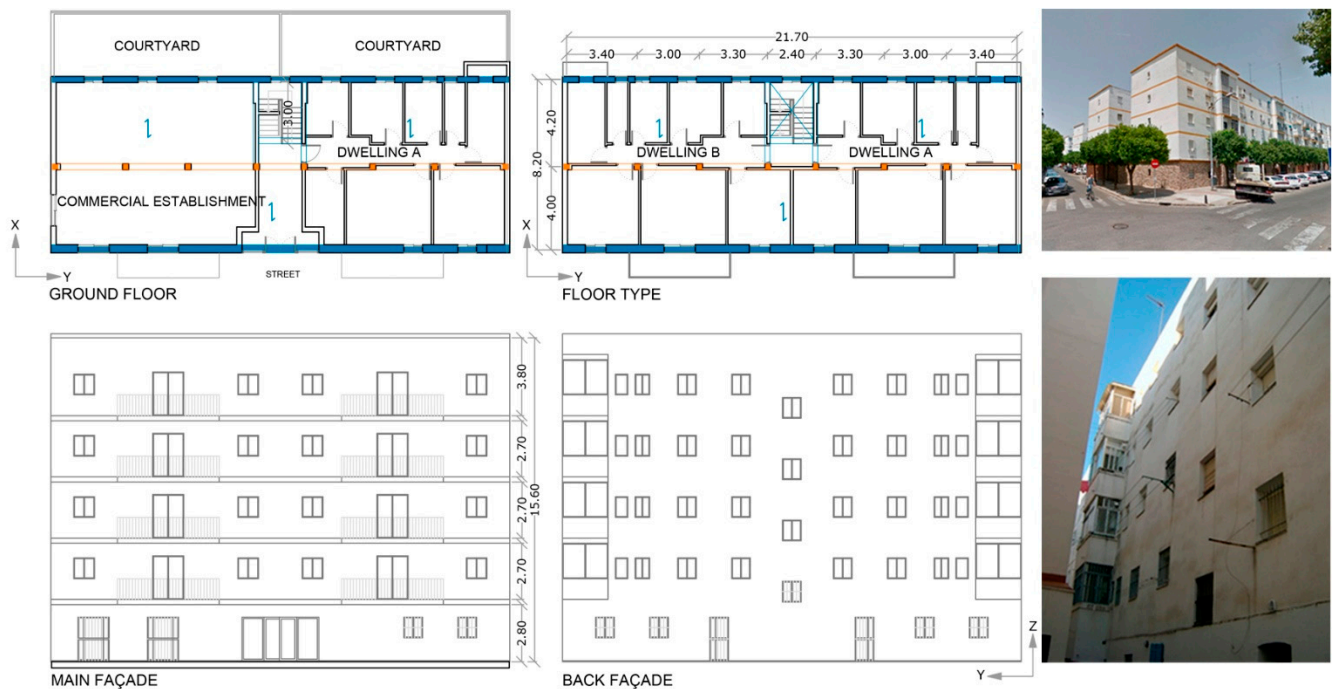


Figure 3. Structural configuration highlighting in blue the masonry walls and, in orange, the interior RC frame. Distribution in plan and elevation. Photos of the building (by the authors).

2.2.2. Energetic Characterisation

The configuration of the envelope (Table 2) is representative of neighbourhoods constructed during the 1960s–1970s in Andalusia. It is typified by the absence of thermal insulation and the numerous thermal bridges in the joints of the façade (Figure 4). The openings were constructed with sliding-type windows, aluminium frames without thermal breaks, and single glazing with an exterior roller shutter.

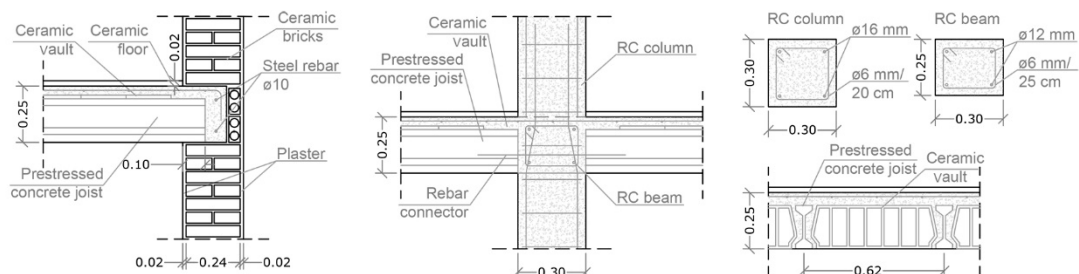


Figure 4. Constructive and structural details of the building.

Table 2. Constructive building characterisation.

| | Composition | Transmittance U (W/m ² K) | Solar Factor |
|----------------------------|---|---|--------------|
| Façade | Cement mortar (2 cm); one foot of hollow metric brick ‘gafa type’ (24 cm); cladding of plaster (1 cm). | 1.74 | - |
| Façade of the ground floor | Foot and a half of solid metric brick (36 cm); cladding of plaster (1 cm). | 1.54 | - |
| Floor slab | Terrazzo floor (2 cm); cement mortar (3 cm); jack arch brick one-way spanning slab (25 cm); cladding of plaster (1.5 cm). | 1.57 | - |
| Roof | Pressed brick flooring (0.8 cm); cement mortar (1.5 cm); lost flooring (0.8 cm); lightweight aggregate concrete, formation of slope (mean 5 cm); jack arch brick one-way spanning slab (25 cm); cladding of plaster (1.5 cm). | 1.59 | - |
| Ground floor | Terrazzo floor (2 cm); cement mortar (3 cm); conventional solid concrete slab (10 cm) | 1.24 | - |
| Windows | Aluminium frame with no thermal break; single glass pane (6 mm) | 5.70 | 0.83 |

3. Energy and Seismic Performance of the As-Built Building

3.1. Seismic Performance Assessment

3.1.1. Numerical Modelling

The numerical models for the seismic assessment have been developed using the OpenSees finite element (FE) software framework [43]. An STKO pre-/postprocessor [44] and Matlab [45] were used to graphically visualise and to handle the outputs, respectively. A load-control NLS analysis of the structure was performed, considering a triangular load pattern. This is the most restrictive load pattern, which is computed according to the masses at each floor and height [7]. The control node is located at the centre of masses of the top floor.

There are several approaches to model URM structures. These were reviewed and classified in [46]. In this work, the numerical modelling of the structure was performed following the equivalent frame (EF) method [47]. This method idealises masonry walls as piers (vertical panels) and spandrels (horizontal panels) connected by rigid areas (where no seismic damage was observed after seismic events [48]). Macroelements were developed to model the URM panels considering the distributed plasticity approach, validated in a previous work developed by the authors [49]. A force-based element (FBE) with fibre cross sections were defined following the prescriptions established in [50]. These macroelements are able to predict the in-plane and the out-of-plane behaviour of the panels as well as the bending and the shear behaviours. Masonry nonlinearity was defined according to a uniaxial stress–strain law along the frame using the ‘Concrete02’ uniaxial material. A phenomenological shear force–deformation (V – γ) law was defined to account for shear, according to the prescriptions established in [50]. Different values of maximum interstorey drift were defined for the spandrels modelling and considering the experimental results obtained by [51]. The maximum strength of the panels (V_y) was computed according to the well-known Turnšek and Čačovič criterion [52] to account for the diagonal cracking. V_y is evaluated according to the acting axial load (N) in panels at each step. N varies during the analyses, owing to the redistribution phenomena. Note that in OpenSees, this is not automatically computed compared with other URM-wall-specific software. To overcome this limitation, and as suggested by [49,50], it has been decided to set at the beginning of the analyses the results from the gravitational loads applied at nodes. RC frames were modelled with the FBE and the distributed plasticity approach using the ‘Concrete02’ uniaxial, as already followed by the authors in [7]. More information on the modelling

of the URM walls for this case study structure can be found in the previous works of the authors [49].

3.1.2. Seismic Safety Criteria

Once the capacity has been obtained, the seismic safety has been verified using the capacity/demand ratio (CDR). The CDR is expressed as the division of the seismic expected damage divided by the seismic demand displacement (d_{dem}). In this work, the severe damage limit state (LS) was considered for the seismic damage assessment (d_{SD-i}), as suggested by EC8. In order to comply with the seismic safety verification, the CDR should be higher than 1. For the computation, the average between the X- and Y-direction values was considered.

In order to exhaustively assess the local damage in URM walls, the usability-preventing damage (UPD) LS, specifically developed in [53] for URM walls, was considered. Hence, in this work, the d_{SD-I} from EC8 was computed following the criteria established for the UPD LS. Since the in-box behaviour of the structure is guaranteed owing to the horizontal connections, only the in-plane failure is borne in mind in the damage assessment. In order to compute the UPD LS, the criteria established in [53] was followed, which states that the UPD LS is attained when: (i) 50% of the masonry walls present light-widespread damage, (ii) one masonry wall reaches a 40% drop of V_y in the case of the phenomenological nonlinear beam, and (iii) the attainment of 95% of the maximum V_b of the structure. In addition, the UPD LS threshold should not be lower than 85% of the peak resistance since URM walls can present slight but widespread damage at values far from peak resistance.

For the seismic demand assessment, the results obtained by the NLS analysis were used in conjunction with the N2 method to estimate the performance of the structure. As this method can lead to a certain level of inaccuracy if applied to URM buildings, dynamic analyses are recommended. However, for this study, the N2 method and NLS analyses are used as an initial seismic assessment and for the rapid design of possible retrofitting solutions, as inaccuracies are not expected to be notable. For the UPD LS, the ground motion return period is 475 years according to EC8. For the location of the building, the seismic action is equal to 0.1 g, and the importance factor is 1.

3.1.3. Preliminary Seismic Assessment of the As-Built Structure

Before the design of the alternative retrofitting solutions, the performance of the as-built structure was assessed. The results of the modal analysis of the as-built structure are shown in Figure 5. As can be observed, Modes 1 and 2 are mainly translational in the X-direction (red axis) and Y-direction (green axis), respectively. Mode 3 is rotational in the X- and Y-directions, having a 30% of participation masses in each direction.

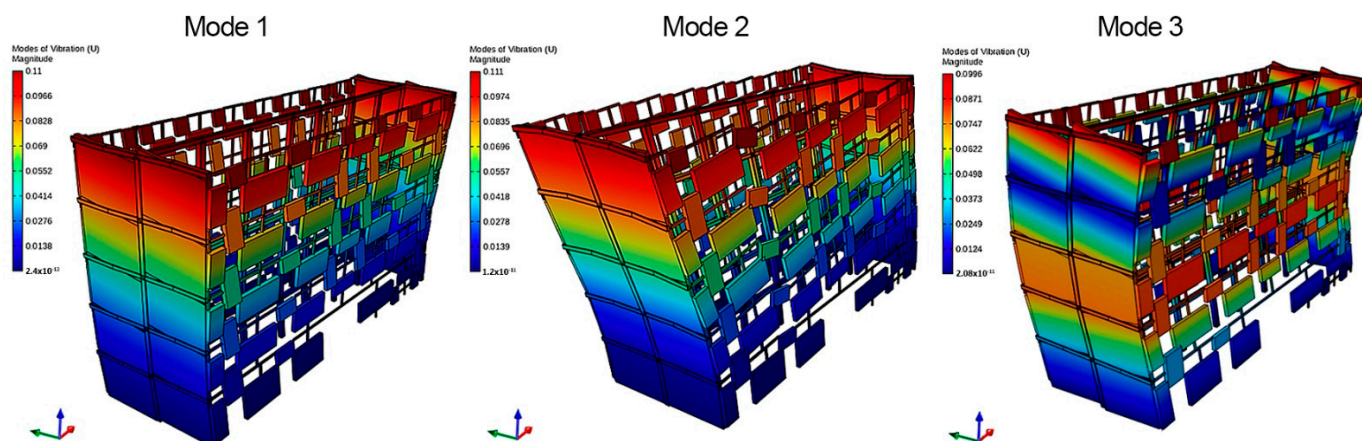


Figure 5. Modal shapes of the case study according to the first three modes of vibration.

The results of NLS analyses are expressed in terms of single-degree-of-freedom (SDOF) capacity curves, normalised by dividing the shear force at the base (V_b) and the top displacement (d_{top}) by the total weight (W_t) and height (h_t) of the building. As observed in Figure 6a, the behaviour of the building in the X-direction is more brittle than in the Y-direction due to the presence of the main URM walls. Considering the CDR assessment, it was obtained that the building will not comply with the seismic safety verification since the ratio will be 0.79. Specifically, the ratios obtained for the X- and Y-directions were 0.53 and 1.05, respectively. The expected seismic damage in each wall of both the main and the back façade for the seismic demand step is shown in Figure 6b. It was obtained that the most affected walls are those located on the ground floor. The different types of expected damage were computed according to the work developed in [49], considering the interstorey drift limits from the constitutive shear and flexural laws of each panel.

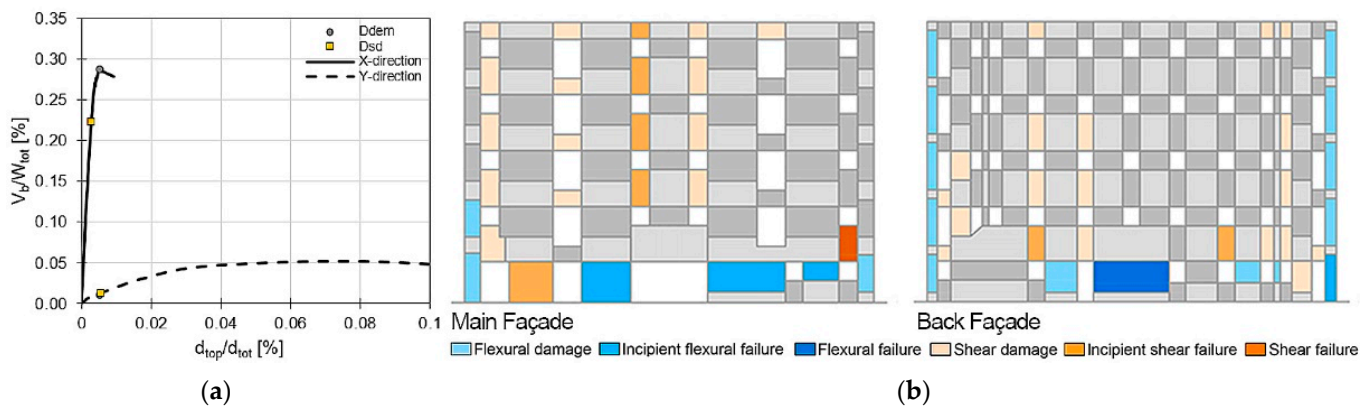


Figure 6. (a) Normalised SDOF-NLS curves plotting both the seismic demand (d_{dem}) and the SD LS (d_{SD}) for the as-built structure. (b) Damage at each single wall for the main and the back façade for the seismic demand step and the as-built condition.

3.2. Energy Performance Assessment

3.2.1. Numerical Modelling

The models for the energy performance simulation were generated and evaluated using a technical software called CYPE. First, the IFC Builder plugging was used to create the IFC model of the building. Then, CYPETHERM HE plus (CTE 2019) (Version 9.5) [54], a computational tool based on the validated EnergyPlus™ calculation (recognised by the Spanish ministry), was employed to obtain the current annual energy demand. Different variations of the energy simulation model were carried out to take into account the retrofitting strategies proposed. The model developed in the software is shown in Figure 7, where both the main and the back façade can be observed.

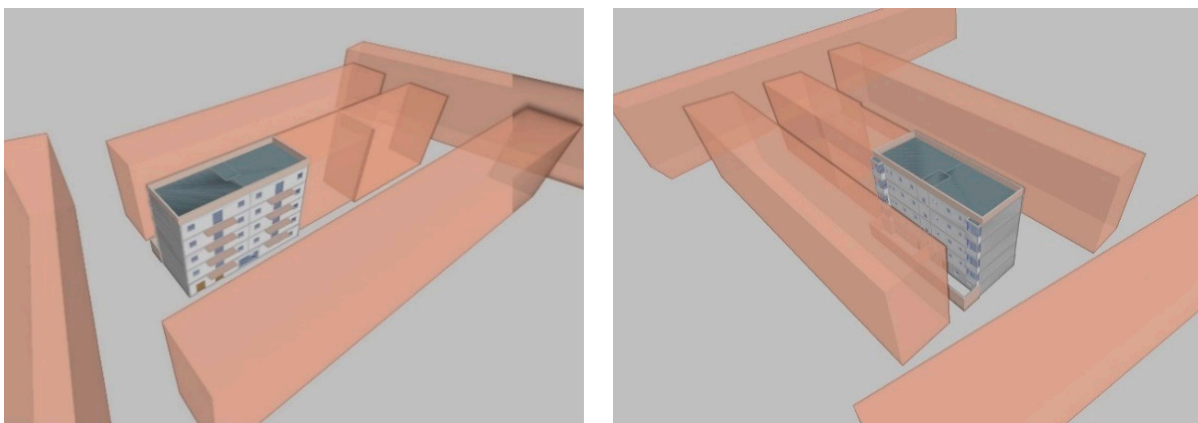


Figure 7. Model developed for the energy performance assessment in 3D.

3.2.2. Configuration of the Simulation

The Spanish Building Technical Code (CTE) [55] establishes different climatic zones according to climatic severity in winter (SCI) and in summer (SCV). The climatic zone corresponding to the city of Seville is B4, which refers to a climate that is mild in winter and very warm in summer [56]. In this work, this climatic zone was considered for the analyses and the meteorological data template named as Spanish weather for energy calculations [57]. The simulation conditions established in Table 3 were defined according to the Spanish energy standards [56,58]. The operating conditions were uniformly applied to dwellings, modelling each one as a single enclosure (only considering its delimiting parameters). The distribution areas were considered unconditioned spaces, assuming a heating transfer within their inner divisions. The input data related to the ventilation was defined according to [59], assuming 1.25 ac/h throughout the year and 4 ac/h from 00:00 to 08:00 local time in summer. Thermal bridges were introduced according to the Spanish building code regulations [60].

Table 3. Energetic simulation conditions.

| | 1–7 h | 8 h | 9–15 h | 16–18 h | 19 h | 20–23 h | 24 h |
|--|-------|------|--------|---------|------|---------|------|
| Cooling | | | | | | | |
| January to May (°C) | - | - | - | - | - | - | - |
| June to September (°C) | 27 | - | - | 25 | 25 | 25 | 27 |
| October to December (°C) | - | - | - | - | - | - | - |
| Heating | | | | | | | |
| January to May (°C) | 17 | 20 | 20 | 20 | 20 | 20 | 17 |
| June to September (°C) | - | - | - | - | - | - | - |
| October to December (°C) | 17 | 20 | 20 | 20 | 20 | 20 | 17 |
| Sensitive loads due to occupation | | | | | | | |
| Weekdays (W/m ²) | 2.15 | 0.54 | 0.54 | 1.08 | 1.08 | 1.08 | 2.15 |
| Weekend (W/m ²) | 2.15 | 2.15 | 2.15 | 2.15 | 2.15 | 2.15 | 2.15 |
| Latent loads due to occupation | | | | | | | |
| Weekdays (W/m ²) | 1.36 | 0.34 | 0.34 | 0.68 | 0.68 | 0.68 | 1.36 |
| Weekend (W/m ²) | 1.36 | 1.36 | 1.36 | 1.36 | 1.36 | 1.36 | 1.36 |
| Sensitive loads due to lighting equipment | | | | | | | |
| Every day (W/m ²) | 0.44 | 1.32 | 1.32 | 1.32 | 2.20 | 4.40 | 2.20 |
| Sensitive loads due to electronic equipment | | | | | | | |
| Every day (W/m ²) | 0.44 | 1.32 | 1.32 | 1.32 | 2.20 | 4.40 | 2.20 |
| Ventilation | | | | | | | |
| January to May (ac/h) | 1.25 | 1.25 | 1.25 | 1.25 | 1.25 | 1.25 | 1.25 |
| June to September (ac/h) | 4.00 | 4.00 | 1.25 | 1.25 | 1.25 | 1.25 | 1.25 |
| October to December (ac/h) | 1.25 | 1.25 | 1.25 | 1.25 | 1.25 | 1.25 | 1.25 |
| Hot water utilisation at 60 °C | | | | | | | |
| Every day (L/m ²) | 0.00 | 0.26 | 0.065 | 0.065 | 0.13 | 0.26 | 0.00 |

The airtightness level of buildings significantly affects the energy consumption and indoor temperatures in dwellings. In this work, the prediction and definition of the n_{50} value (air infiltration rate at 50 Pa) in buildings was computed according to [61]. The equation resulting from the predictive model developed to define the airtightness of multifamily buildings in the Mediterranean region was used. In this case, Model 2 was considered (airtightness calculation in dwellings built before 1979). As a result, an n_{50} value of 9.6 was obtained for the as-built condition. This value is in agreement with the measures taken in different studies carried out in buildings of similar characteristics in Seville [61]. The EnergyPlus™ computational model of the building is validated by comparing and calibrating these results simulated with the values measured experimentally in a previous

exhaustive campaign carried out in the region of Andalusia (in social housing of similar characteristics) within the framework of the regional Efficacia project [62].

3.2.3. Preliminary Energy Assessment of the As-Built Structure

The results of the preliminary energy assessment concluded that in all the possible four different orientations of the block, the heating demand is much higher than that of cooling (Figure 8). These results are contrary to what would initially be expected for a climatic area with warm summers. However, the proportion of urban canyon favours the mutual shading of the buildings, largely avoiding direct solar radiation on the façades of the blocks. Similar results were obtained in social housing analyses in this city by [63]. As shown in Table 4, no significant differences in the energy demand values can be found, considering the orientations of the blocks (NE, SW, NW, SE). Similarly, when performing detailed analyses of the dwellings, no significant differences are found between dwellings on the same floor (Figure 9). This is mainly because of the typology of the block: two dwellings per floor and a double façade. However, variations between floors can be observed, resulting in a higher demand required by the upper floors. Parameters A and B refer to the two dwellings that the building presents per floor.

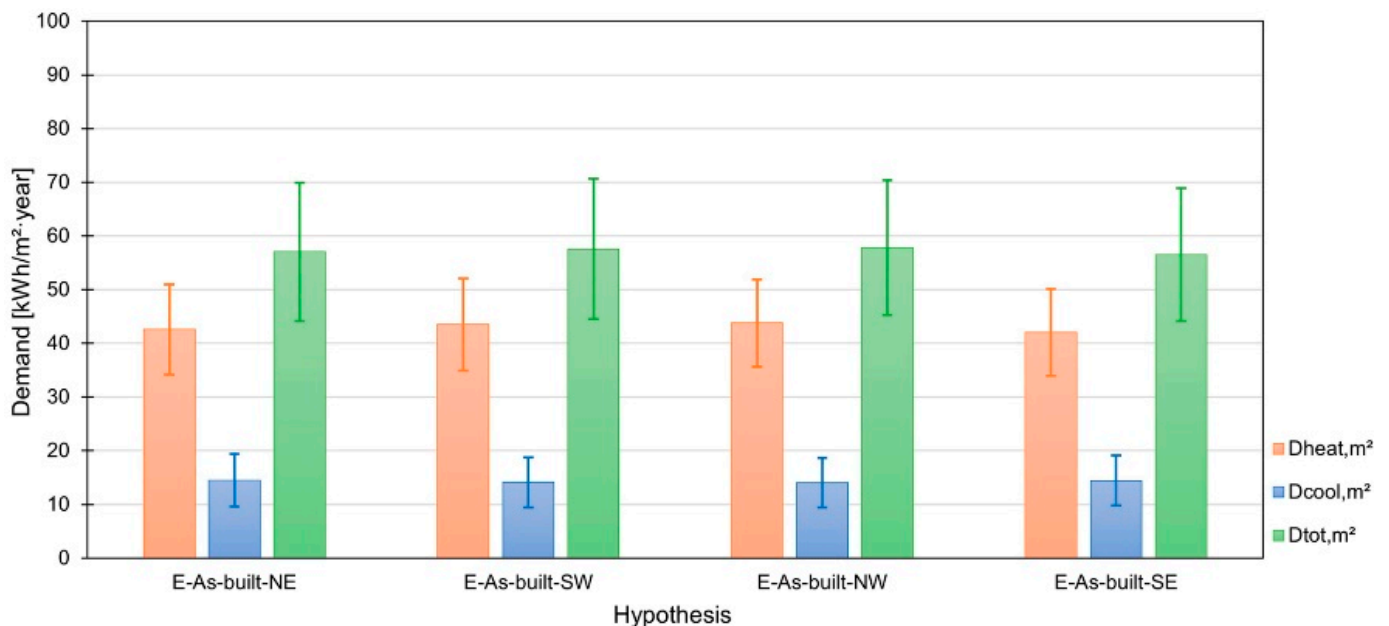


Figure 8. Annual average thermal demand values per m² according to orientation.

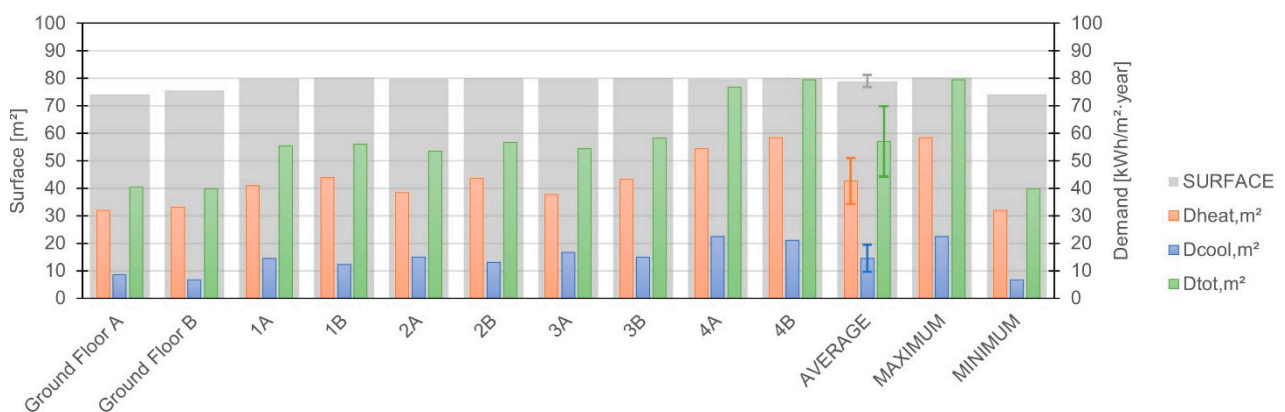


Figure 9. Dwelling annual thermal demand for the as-built hypothesis, including the surface of each dwelling.

Table 4. Annual thermal demand values obtained for the as-built configuration.

| | AVERAGE | | | AVERAGE | | | AVERAGE | | |
|--------------|----------------------------|----------------------------|----------------------------|----------------------------|----------------------------|----------------------------|----------------------------|----------------------------|----------------------------|
| | Dheat, m ² | Dcool, m ² | Dtot, m ² | Dheat, m ² | Dcool, m ² | Dtot, m ² | Dheat, m ² | Dcool, m ² | Dtot, m ² |
| | (kWh/m ² ·year) |
| E-Asbuilt-NE | 42.55 | 14.49 | 57.04 | 58.35 | 22.50 | 79.44 | 31.85 | 6.55 | 39.72 |
| E-Asbuilt-SW | 43.48 | 14.08 | 57.57 | 59.27 | 21.51 | 79.68 | 32.69 | 6.54 | 39.76 |
| E-Asbuilt-NW | 43.77 | 14.02 | 57.79 | 58.40 | 21.33 | 78.66 | 32.72 | 6.51 | 39.93 |
| E-Asbuilt-SE | 42.06 | 14.44 | 56.50 | 57.57 | 21.92 | 78.08 | 31.86 | 6.66 | 39.79 |

4. Integrated Seismic and Energy Retrofitting Interventions

4.1. Description of the Solutions Proposed and Sensitivity Analysis

Strategies were based on the behaviour of the as-built state. The building is expected to present in-plane failure owing to the presence of horizontal connections. Furthermore, it was observed from the as-built assessment that the façades of the building lead to higher ratios of heating transfer. Given this, both energy and seismic retrofitting strategies are applied to enhance the façade elements or wall behaviour. It is worth mentioning the importance of the roof in the energy performance. However, since the objective of this work is to propose integrated energy and seismic retrofitting solutions, the modification of the roof will not be taken into account. As obtained from the as-built assessment, the internal RC frame does not require seismic strengthening interventions.

Hence, with reference to the case study building, different retrofitting packages (RP) were proposed. These are focused on improving the performance of two main aspects of the façade of the URM buildings, which affect both the seismic and energy performance. Moreover, these are two of the most implemented energetic solutions in buildings [12,22]: openings (RP₁) and walls (RP₂). Additionally, an RP₃ was proposed by combining solutions from previous RPs. The solutions selected are to be combined and integrated. Their conceptual designs are shown in Figure 10. The goal is to design and analyse one-shot interventions that can help reduce economic costs, while retaining acceptable performance targets.



Figure 10. Conceptual details of the retrofitting packages: wall strengthening and addition of thermal insulation and addition of encirclements and window replacement/enhancement.

Based on each RP, different solutions were proposed. In the case of seismic performance, RP₁ is based on the addition of encirclements in openings. For the energy performance enhancement, solutions focused on the replacement/enhancement of windows (both glazing and frames). RP₂ proposes adding steel grids on URM walls to improve their seismic performance. For the energy enhancement, thermal insulation was added to walls. In order to analyse the influence of each retrofitting technique, a sensitivity analysis was carried out. Different models were defined by varying certain parameters according to the seismic or energy behaviour. These are described below. The models analysed are listed in Table 5. In total, 24 and 48 configurations were assessed for the seismic and energy

performance enhancement, respectively. The nomenclature of each abbreviation (Ab) is defined in its corresponding section.

Table 5. Models defined for the sensitivity analysis.

| Seismic Performance | | | | Energy Performance | | | |
|---------------------|-------|-----------------|-------|--------------------|---------|-----------------|---------|
| RP ₁ | | RP ₂ | | RP ₁ | | RP ₂ | |
| Extended | Ab. | Extended | Ab. | Extended | Ab. | Extended | Ab. |
| RP1-L-60-1 | S-W1 | RP2-15-6-1 | S-F1 | RP1-AL-STA-NE | E-W1-NE | RP2-EPS-5-NE | E-F1-NE |
| RP1-L-60-2 | S-W2 | RP2-15-8-1 | S-F2 | RP1-AL-STA-SW | E-W1-SW | RP2-EPS-5-SW | E-F1-SW |
| RP1-L-90-1 | S-W3 | RP2-20-6-1 | S-F3 | RP1-AL-STA-NW | E-W1-NW | RP2-EPS-5-NW | E-F1-NW |
| RP1-L-90-2 | S-W4 | RP2-20-8-1 | S-F4 | RP1-AL-STA-SE | E-W1-SE | RP2-EPS-5-SE | E-F1-SE |
| RP1-L-120-1 | S-W5 | RP2-30-6-1 | S-F5 | RP1-AL-LEM-NE | E-W2-NE | RP2-EPS-10-NE | E-F2-NE |
| RP1-L-120-2 | S-W6 | RP2-30-8-1 | S-F6 | RP1-AL-LEM-SW | E-W2-SW | RP2-EPS-10-SW | E-F2-SW |
| RP1-O-60-1 | S-W7 | RP2-15-6-2 | S-F7 | RP1-AL-LEM-NW | E-W2-NW | RP2-EPS-10-NW | E-F2-NW |
| RP1-O-60-2 | S-W8 | RP2-15-8-2 | S-F8 | RP1-AL-LEM-SE | E-W2-SE | RP2-EPS-10-SE | E-F2-SE |
| RP1-O-90-1 | S-W9 | RP2-20-6-2 | S-F9 | RP1-WOOD-STA-NE | E-W3-NE | RP2-EPS-5-10-NE | E-F3-NE |
| RP1-O-90-2 | S-W10 | RP2-20-8-2 | S-F10 | RP1-WOOD-STA-SW | E-W3-SW | RP2-EPS-5-10-SW | E-F3-SW |
| RP1-O-120-1 | S-W11 | RP2-30-6-2 | S-F11 | RP1-WOOD-STA-NW | E-W3-NW | RP2-EPS-5-10-NW | E-F3-NW |
| RP1-O-120-2 | S-W12 | RP2-30-8-2 | S-F12 | RP1-WOOD-STA-SE | E-W3-SE | RP2-EPS-5-10-SE | E-F3-SE |
| | | | | RP1-WOOD-LEM-NE | E-W4-NE | RP2-RW-5-NE | E-F4-NE |
| | | | | RP1-WOOD-LEM-SW | E-W4-SW | RP2-RW-5-SW | E-F4-SW |
| | | | | RP1-WOOD-LEM-NW | E-W4-NW | RP2-RW-5-NW | E-F4-NW |
| | | | | RP1-WOOD-LEM-SE | E-W4-SE | RP2-RW-5-SE | E-F4-SE |
| | | | | RP1-PVC-STA-NE | E-W5-NE | RP2-RW-10-NE | E-F5-NE |
| | | | | RP1-PVC-STA-SW | E-W5-SW | RP2-RW-10-SW | E-F5-SW |
| | | | | RP1-PVC-STA-NW | E-W5-NW | RP2-RW-10-NW | E-F5-NW |
| | | | | RP1-PVC-STA-SE | E-W5-SE | RP2-RW-10-SE | E-F5-SE |
| | | | | RP1-PVC-LEM-NE | E-W6-NE | RP2-RW-5-10-NE | E-F6-NE |
| | | | | RP1-PVC-LEM-SW | E-W6-SW | RP2-RW-5-10-SW | E-F6-SW |
| | | | | RP1-PVC-LEM-NW | E-W6-NW | RP2-RW-5-10-NW | E-F6-NW |
| | | | | RP1-PVC-LEM-SE | E-W6-SE | RP2-RW-5-10-SE | E-F6-SE |

4.2. Proposed Seismic Retrofitting Solutions and Numerical Modelling

In the case of the seismic (S) behaviour improvement, the sensitivity analysis was based on varying three parameters: (i) the amount of reinforcing material, (ii) the type of reinforcing materials, and (iii) the type of reinforcing elements. For (i), the width, the spacing, and the thickness of the retrofitting elements were varied. For (ii), the structural steel type was varied. For (iii), the type of profiles added to openings was changed. In Table 6, the different configurations modelled are listed and described. The nomenclature of each model is defined according to the abbreviations in bold.

Table 6. Parameters varied in the sensitivity analysis of the seismic behaviour.

| | S-RP ₁ | S-RP ₂ |
|------------------------------------|--|--|
| (i) Amount of reinforcing material | L-profile 60.5.8/90.10.11/120.10.13 | Spacing: 15/20/30 mm |
| (ii) Type of reinforcing materials | O-profile 60.2/90.5/120.4 | Dimension: ϕ 6/ ϕ 8 mm |
| (iii) Type of reinforcing elements | $f_y = 235$ (1)/275 (2) MPa | $f_y = 235$ (1)/275 (2) MPa |
| | L-profile/ O -profile | |

The numerical simulation of each technique in OpenSees was developed as follows. S-RP₁ (addition of a steel profile in the openings) was modelled by adding frame elements connected to the walls with rigid element links. Frames were modelled with FBE. S-RP₂ (addition of a steel mesh) was modelled by modifying the constitutive laws of the panels according to the amount of retrofitting material added. The procedure and formulae presented in [64] to account for the addition of retrofitting materials in URM macroele-

ments were followed. The properties of the structural steel of the retrofitting elements are: $E = 210$ GPa and $W = 76.98$ kN/m³.

4.3. Energy Retrofitting Solutions Proposed and Numerical Modelling

For the energy (E) performance enhancement, different hypotheses were defined by varying some parameters in the sensitivity analysis. These are established in Table 7. E-RP₁ is based on improving the thermal transmittance and airtightness of the openings. Different models were defined by varying the frame material and the glass composition. E-RP₂ focused on improving the thermal transmittance of the opaque envelope. To do so, different models were defined by varying the material of the external thermal insulating composite system (ETICS) and the thickness of the insulation. In addition, based on the results obtained in previous studies [12], a third hypothesis is introduced in which the insulation thickness varies according to the orientation of each façade (south-facing façades, one thickness, and north-facing façades, another). This is proposed to analyse the improvement of the possible imbalance of demand requirements due to the homogeneous treatment of the different façades.

Table 7. Models analysed in the sensitivity analysis of the energy behaviour.

| | | Material (Transmittance U (W/m ² K)) | Properties (Transmittance U (W/m ² K)) | Transmittance U (W/m ² K) | Solar Factor |
|-------------------|----|--|---|---|--------------|
| As-built | W0 | Aluminium (no thermal bridge break) (5.70) | 4 mm single glass (5.70) | - | 0.83 |
| E-RP ₁ | W1 | Aluminium | 4/6/4 normal glass (3.30) | - | 0.75 |
| | W2 | w/thermal bridge break (2.80) | 4/6/4 low-e glass (2.50) | - | 0.48 |
| | W3 | Wood | 4/6/4 normal glass (3.30) | - | 0.75 |
| | W4 | (1.43) | 4/6/4 low-e glass (2.50) | - | 0.48 |
| | W5 | PVC | 4/6/4 normal glass (3.30) | - | 0.75 |
| | W6 | (2.30) | 4/6/4 low-e glass (2.50) | - | 0.48 |
| As-built | F0 | - | - | 1.74 | - |
| E-RP ₂ | F1 | Expanded polystyrene styroboard | 5 cm | 0.51 | - |
| | F2 | (EPS) | 10 cm | 0.31 | - |
| | F3 | (0.037) | Combined | 0.51/0.31 | - |
| | F4 | Rock wool | 5 cm | 0.51 | - |
| | F5 | (0.037) | 10 cm | 0.31 | - |
| | F6 | | Combined | 0.51/0.31 | - |

In all scenarios, the thermal bridges were modified in the simulation model in accordance with the current regulation [60]. Concerning the prediction of the watertightness, when introducing the improvement of façades and/or openings, different assumptions were borne in mind. According to previous studies, it is concluded that the introduction of an ETICS system without touching openings does not introduce important modifications in the infiltrations of the dwelling [61,65]. Contrariwise, the renovation of the windows system produces a reduction of up to 30% to 40% of the n_{50} value [66]. This margin of improvement agrees with the data obtained in [61,67]. The difference in frame materials only implies a substantial change in PVC, while aluminium and wood behave in a similar way [67]. Therefore, based on the data measured in previous studies, the infiltration value remains constant for the E-RP₂ scenarios, and it is modified for that of E-RP₁. The n_{50} value was set to 6.5 for the hypothesis with aluminium and wood frames and to 5.0 for the PVC frames.

4.4. Results of the Sensitivity Analysis

The performance assessment of the models retrofitted was conducted in the same fashion as the as-built structure, denoted as 'As-built'. A model analysis for each solution established in Table 5 was performed to obtain both the seismic and the energy performance.

In the case of the seismic performance, following the modal analyses, NLS analyses were carried out, and the N2 method was used to determine the performance of each solution. In Figure 11, the results for the S-RP₁ technique were plotted. From this figure, it is immediately clear that adding encirclements in walls in one direction (X) does not affect the performance of the models in the other direction (Y). As can be seen, the initial stiffness of the URM system is not significantly affected by the addition of the retrofitting elements. Solutions that added O-profiles led to higher improvements than those that added L-profiles. The implementation of an enhanced steel material leads to a certain improvement of the performance, reaching improvements of up to 5–10% compared with the other steel material. Considerable differences can be observed from adding the smallest profile (either O- or L-profile) to the biggest one, reaching improvements of up to 20%.

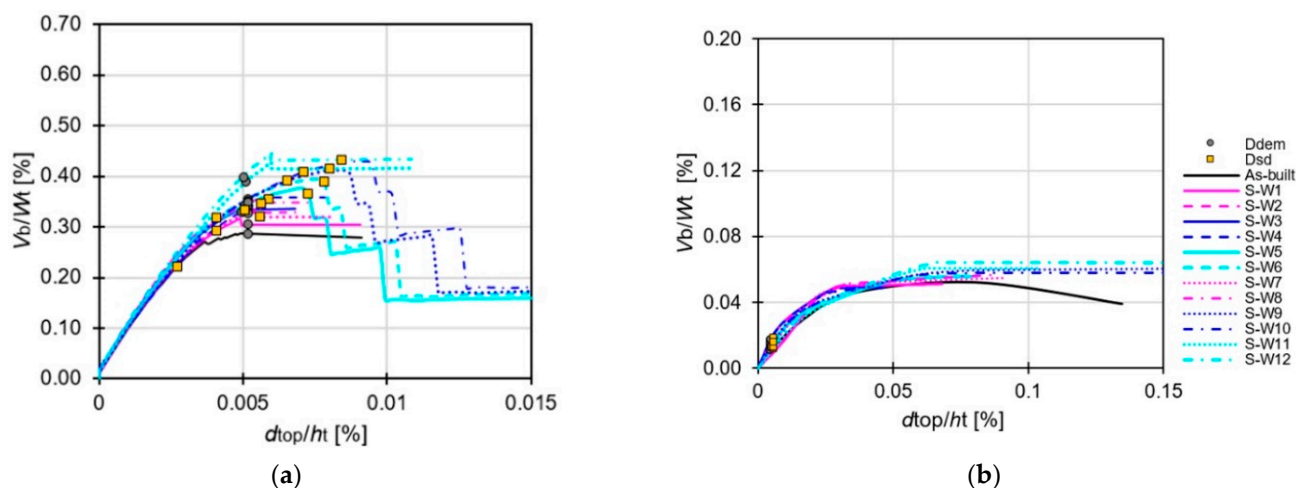


Figure 11. Normalised SDOF-NLS curves considering the S-RP₁ solutions in the X- (a) and Y- (b) direction.

The implementation of steel grids in walls (S-RP₂) has led to higher improvement ratios compared with the addition of encirclements in openings (Figure 12). This is mainly due to the considerable increase in the initial stiffness of the URM system, as observed in the plots. The best results were obtained with the solutions that proposed a smaller separation and enhanced the steel yielding strength. The increase in the diameter of the rebar did not produce a considerable enhancement of the performance. This can be considered negligible. The behaviour of the Y-direction was improved since the walls in this direction were also retrofitted.

In the case of the energy performance assessment, the improvement of the models established in Table 5 compared with the As-built state is analysed. In Figure 13, the average-orientation annual thermal demand results for E-RP₁ and E-RP₂ are plotted. In addition, Figure 14 shows the annual thermal demand deviation per m² compared with the As-built state. These graphs clearly show how the window renovation results in a moderate annual energy improvement of the building. Likewise, the energy performance of the models does not undergo significant changes when the material of the window frames is modified. Finally, the introduction of low-emissivity glazing does not lead to a substantial reduction in the annual energy demand, while it will represent a considerable economic increase, as demonstrated in the following sections.

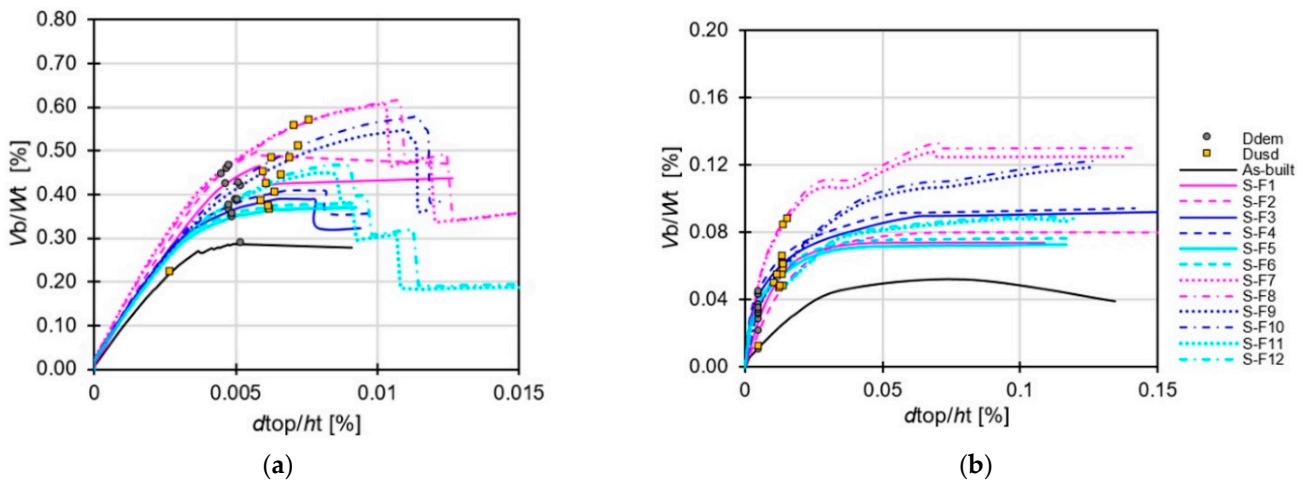


Figure 12. Normalised SDOF-NLS curves considering the S-RP2 solutions in the X- (a) and Y- (b) direction.

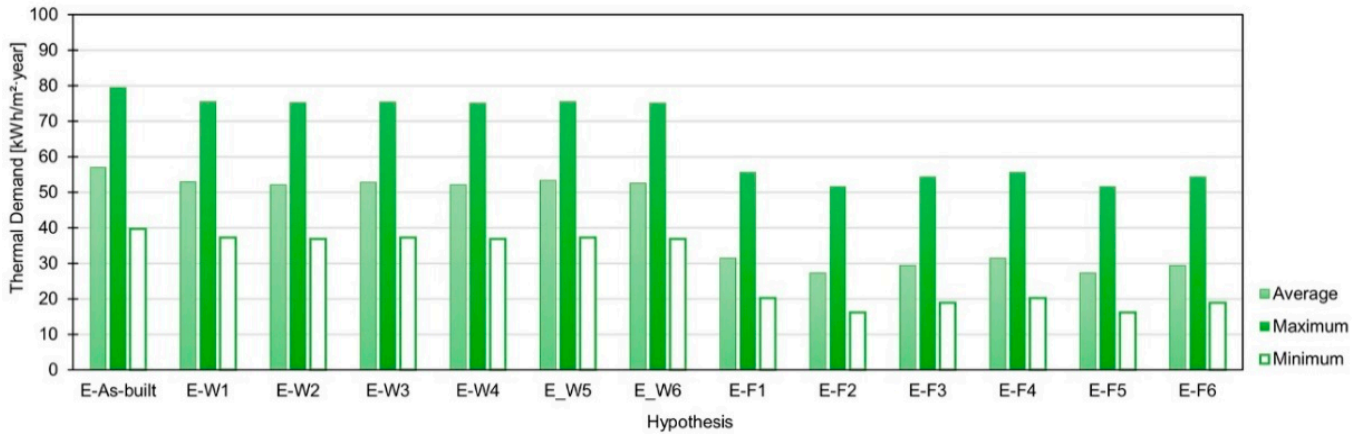


Figure 13. Annual thermal demand per m^2 of the hypothesis (average values of the different orientation models per hypothesis).

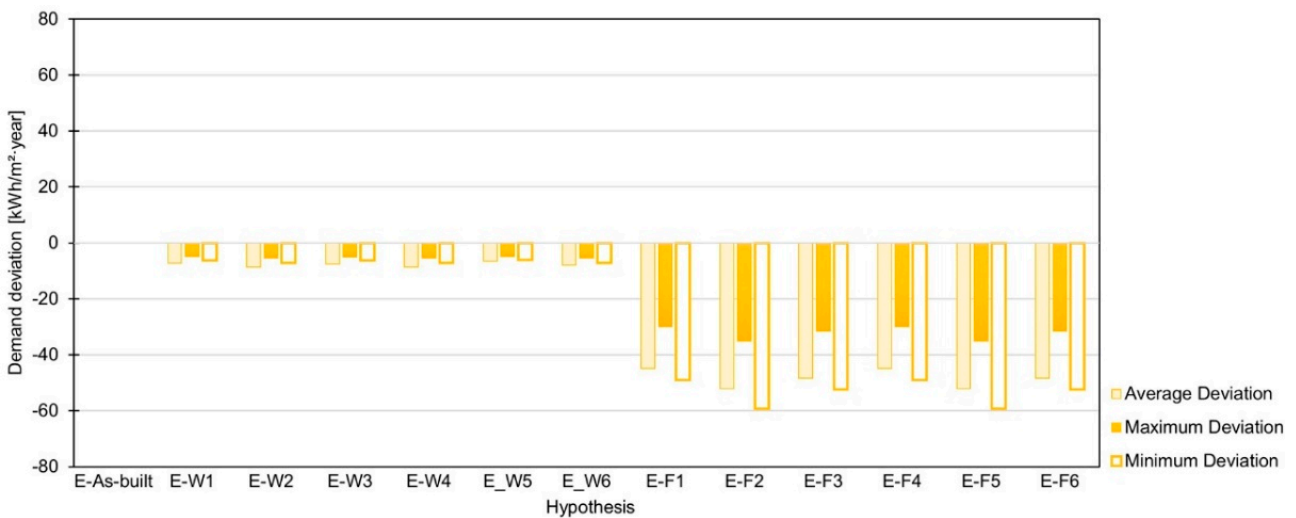


Figure 14. Demand deviation per m^2 (average, maximum, and minimum) regarding the as-built state.

The implementation of thermal insulation in walls led to higher improvements ratios compared with the window renovation (Figures 13 and 14). This is mainly due to the considerable reduction of thermal bridges compared with the as-built state. Thus, the

addition of thermal insulation on the exterior of the façade, in strict compliance with the CTE ($e = 5$ cm) [55], represents a considerable improvement in the energy performance of the building. In fact, it can decrease the annual heating and cooling demand by almost half. As expected, an increase in the thickness of up to 10 cm does not lead to a proportional reduction in the demand. Finally, in line with the results obtained from the as-built state, a detailed treatment of the façades according to the orientation does not introduce an interesting margin of improvement. This happens due to the position of the blocks in the urban configuration (orientation) and the typology of the blocks themselves (double-facing dwellings). Hence, there is no energy imbalance between the different orientations of the dwellings.

4.5. Results of the Benefit–Cost Assessment

The goal of this work is to obtain the most optimal retrofitting configurations to save economic and material resources while producing a considerable performance enhancement. In order to perform the combined energy and seismic assessment, the most optimal solutions were first determined, bearing in mind separately the energy and seismic performance enhancements. In order to select them, a benefit/cost ratio was used, computed as the benefit (B) of each performance divided by the cost (C) of construction. This B/C ratio will allow defining the solutions with the highest improvement ratios and the best costs ratios of both RPs. Once the most optimal individual configurations have been determined for each RP, they have been later combined and integrated.

The cost of the construction of each configuration was computed by means of a bill of quantities and using an updated construction cost database. This database takes into account the duration of the works, the labour and indirect costs, the industrial benefit, and the costs of the materials. A cost index ($C = C_i/C_{exp}$) is determined, expressed as the ratio between the construction cost of the solution analysed (i) and the costs of the most expensive one (exp). This cost index is then used together with the seismic and energy performance improvement ratios. The benefit was computed as the enhancement of the energy and seismic performances. The seismic enhancement ratio ($B_S = d_i/d_{asb}$) is obtained by dividing the CDR of the i solution by the CDR of the as-built state (asb). The energy enhancement ($B_E = E_{asb}/E_i$) is determined by the ratio between the energy demand (kWh/year) of the as-built condition and the demand of the i solution analysed.

In Figure 15, the results of computing the benefit of each RP and the costs of each configuration combined (RP_1 and RP_2) are plotted. C took into account the costs of each RP in order to obtain, for a singular C , two different improvements.

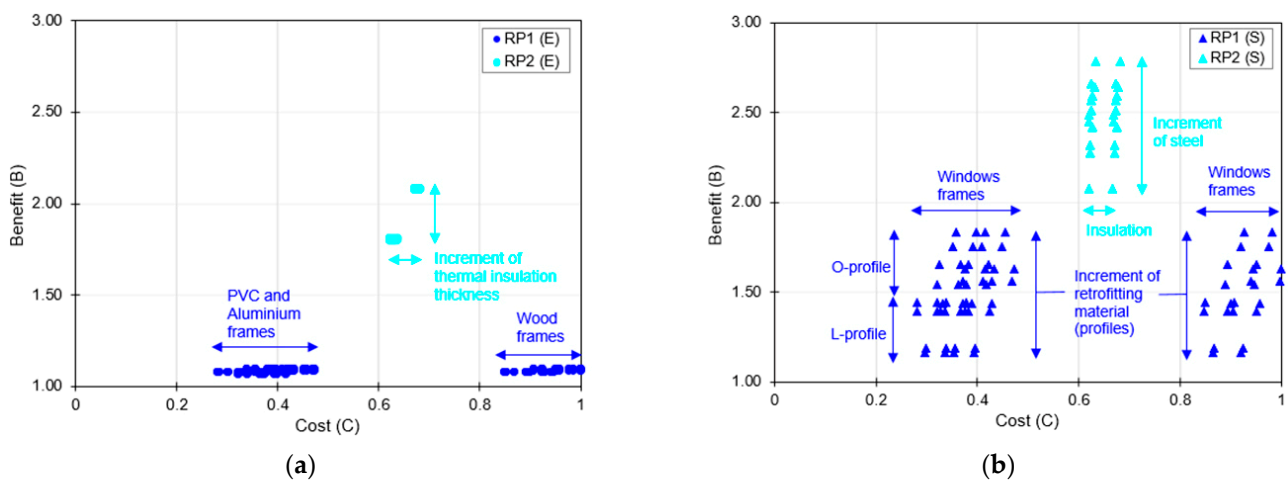


Figure 15. Energy (a) and seismic (b) performance ratios compared with the construction costs of each retrofitting configuration considered.

With regard to the B/C ratio analysis of the different energy-based RP, it can be seen that the highest benefit ratios were obtained for E-RP₂, the addition of an external thermal insulating composite system (ETICS) in walls. E-RP₂ achieved B_E values ranging from 2.56 to 3.13. In the case of E-RP₁, lower values of B_E were obtained, ranging from 1.08 to 1.10. However, E-RP₁ resulted in considerably lower values of C compared with RP₂. Concerning E-RP₁, the results show that two hypothesis groups can be clearly differentiated. The first one encompasses the wooden carpentry solutions, and the other, the aluminium and PVC frames. Despite having similar B_E , wooden frames are significantly more expensive than the other group. In the case of glazing systems, the solutions that include low emissivity glass considerably increase C, providing a negligible B_E .

As regards E-RP₂, the implementation of double insulating thickness material leads to the highest benefits. These solutions are the most profitable ones due to the low increment in costs compared with the outstanding B_E . Changing the type of insulation material, from EPS to rock wool, does not imply a significant variation of the costs or a benefit as both materials present a similar thermal transmittance. Therefore, the solutions with the highest B/C ratio were, from higher to lower, E-W1, E-W5 and E-F2, E-F5. In the case of E-RP₁ solutions, these hypotheses used aluminium and PVC joinery (materials mostly used in residential buildings in Spain due to their optimal energy performance/cost ratio) and standard 4/6/4 double glazing. They obtained similar B_E values while being the cheapest ones. Finally, with regard to E-RP₂, E-F2, and E-F5, these added the highest amount of thermal insulation, which in turn led to these solutions being the most beneficial and optimal ones. As previously obtained in the analysis of the as-built state, the solutions are not considerably affected by the orientation, dwelling typology, and urban situation of the blocks.

The solutions with highest B/C ratios from both RPs were combined and integrated. The results of this combination are plotted in Figure 16. By combining them, the results show that the performance improvements are outstanding compared with the results obtained individually, reaching improvement ratios of up to 336.7%. In total, 16 E-RP₃ configurations were exhaustively assessed.

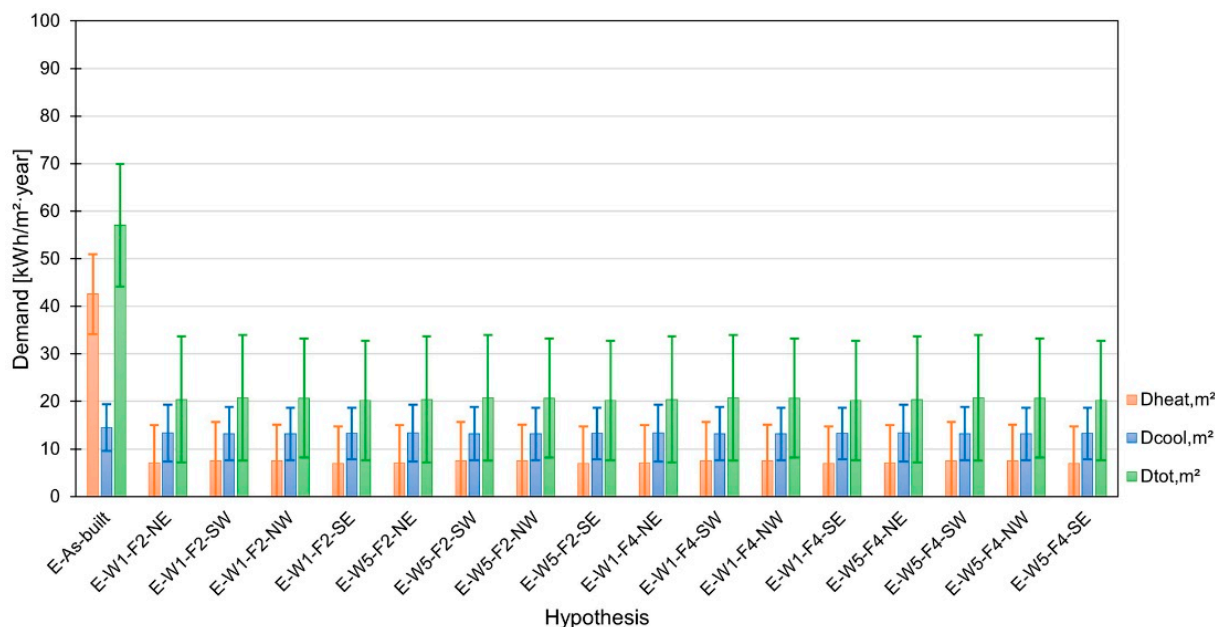


Figure 16. Combination of E-RPs. Annual average thermal demand values per m² according to the orientation of the optimised solutions.

In the case of the seismic enhancement, it can be seen that the highest benefits ratios were obtained for S-RP₂, the addition of steel grids in walls. S-RP₂ achieved B_S values ranging from 2.08 to 2.88. In the case of S-RP₁, lower values of B_S were obtained, ranging

from 1.17 to 1.84. However, this latter S-RP resulted in considerably lower values of C compared with S-RP₂, being up to 70% of C_{RP2} . There are two separated vertical lines that refer to different costs stemming from the increment of thermal insulation. From this first analysis, it was obtained that O-profiles have better benefit and cost ratios than the addition of L-profiles. Additionally, it was obtained that no significant differences can be found in the values of C among all S-RP₂ solutions. However, B_S considerably improves when the amount of material is increased. It was attained that the solutions with the highest B/C ratio were, from higher to lower, S-W8, S-W7, S-W1 and S-F8, S-F7, S-F10. In the case of S-W8 and S-W7, these solutions added the lowest section of O-profiles in openings with different types of steel material. They obtained moderate B_S values, but they were the cheapest solutions. S-W1 is the next cheapest solution. S-F8 and S-F7 added the highest amount of retrofitting steel, resulting in the most beneficial and optimal solutions. S-F10 is the next solution that adds more retrofitting material.

Once the most optimal solutions were determined for each RP assessed separately, they were combined as RP₃. The results of this combination are plotted in Figure 17. In total, nine S-RP₃ configurations were thoroughly assessed. By combining RP₁ and RP₂, the performance improvements were outstanding compared with the results obtained individually, reaching B_S ratios of up to 250%.

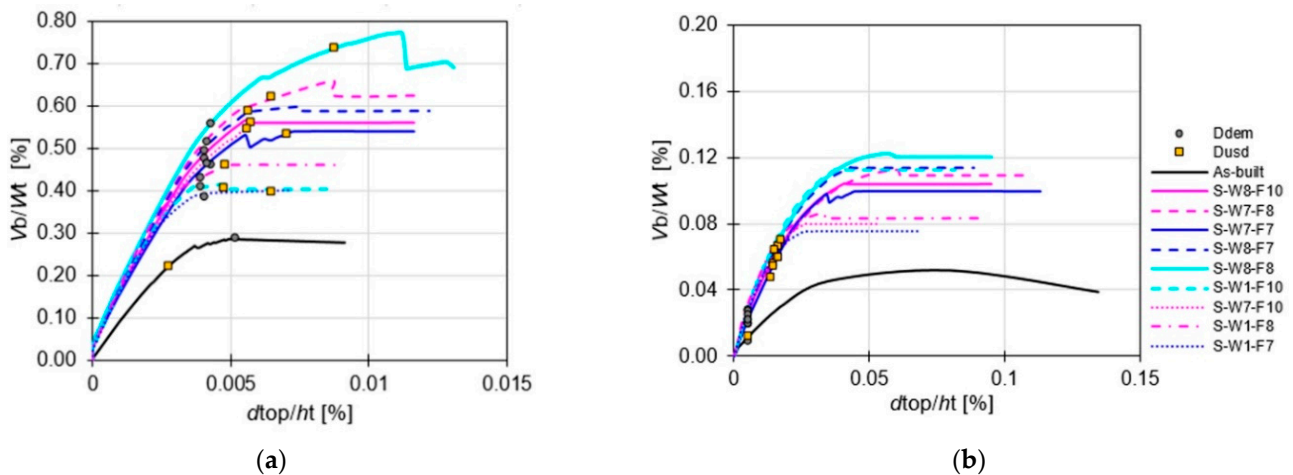


Figure 17. Normalised SDOF-NLS curves considering the RP3 solutions in the X- (a) and Y- directions (b).

4.6. Results of the Combined Energy and Seismic Assessment

In this section, the simultaneous enhancement of the seismic and energy performances and the construction costs are evaluated. The previously carried-out B/C ratio is proposed. In this case, the benefit stemmed from each performance enhancement having been normalised (by dividing the B of each RP configuration by the highest B). This was performed in order to avoid excessive improvement ratios and to establish a similar weight of each performance. The results of the combined assessment, RP₃, are plotted in Figure 18.

When combining the RP and RP₃ configurations, it was obtained that the seismic improvement leads to the highest differences in the results. This is due to the similar energy performance enhancement achieved for all the orientations and hypotheses considered. Nevertheless, the solutions with aluminium window frames and EPS insulation attained higher B/C ratios. In the case of the B_S , there is a considerable difference in the benefit/cost ratio of solutions that add lower and intermediate values of retrofitting material than those that add higher amounts. Significant B_S ratios are obtained if the amount of retrofitting material is increased up to a certain point. In this case, the solutions that presented higher values of B_S were those that added the highest amount of retrofitting material in the walls and those that added the lowest section of O-profiles in the openings. This is due to the negligible values of C among RP₂ solutions and the low C of O-profiles compared with the

moderate benefit ratio. When combined with E-RP, these solutions obtained the highest benefit/cost ratios.

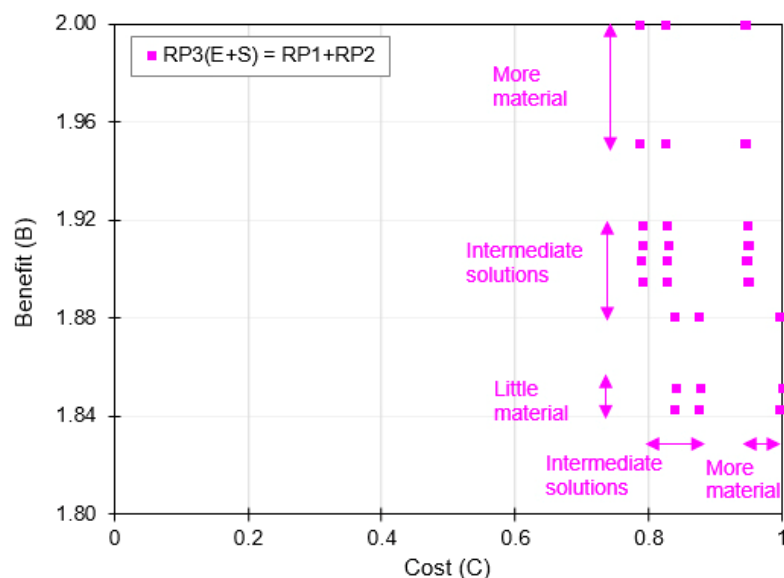


Figure 18. Combined energy and seismic benefit and cost of each integrated RP3 retrofitting configuration considered.

5. Conclusions

This work dealt with the assessment of new integrated and combined seismic and energy retrofitting techniques specifically defined for existing URM buildings. To do so, the solutions were designed for a case study (that does not comply with the seismic and energy demand of the current legislation), and the energy and seismic assessment of its as-built state was also determined. The RPs proposed focused on the improvement of the seismic and energy performance of walls and openings. The novelty of this work is based on the design of one-shot, compatible, noninvasive, and complementary energy and seismic retrofitting solutions applied to the façades of buildings, bearing in mind: the urban environment effects, the achievable seismic and energy performance targets (prescribed by codes in force), and the reduction of costs. The sensitivity analysis enabled assessing the effects of adding each solution. The benefit/cost ratio allowed for obtaining the most optimal configurations to perform the combination and integration of solutions from both RPs and to rank the solutions.

The results of the seismic performance assessment showed that the highest benefit ratio was obtained for S-RP₂, the addition of steel grids in walls. O-profiles have better benefit and cost ratios than the addition of L-profiles. Additionally, it was obtained that no significant differences can be found in the values of C among all the S-RP₂ solutions. Enhanced steel material leads to an increase in performance by 5–10% compared with regular steel material. The increase in the diameter of the rebar in steel grids in walls did not produce considerable enhancement ratios. In the case of S-RP₁, the most optimal solutions were those that added greater retrofitting materials. Similar conclusions were obtained for RP₂. However, in that case, this is due to the negligible differences in the costs among these solutions. The results obtained for the individual assessment were later observed in the combined assessment, RP₃.

The results of the energy performance assessment showed that the introduction of exterior insulation in walls is the technique with the highest impact on the thermoenergetic behaviour of dwellings. Even if a minimum insulation thickness is added, in strict compliance with the CTE, the improvement is substantial. Therefore, it is concluded that for refurbishment activities in residential buildings subjected to reduced budgets, E-RP₂, the improvement of the wall behaviour, seems to be the most profitable solution, despite

the highest economic effort at the beginning. This conclusion is also applied to the seismic performance enhancement. Focusing on the case under study, it was obtained that the orientations, the building typologies, the height-to-width canyon ratios, and the urban situation do not affect the thermal behaviour of the dwellings in the neighbourhood. However, these factors affect the dwellings per floor within the same block. The window renovation without improving the façade behaviour does not imply a significant enhancement in the thermal, energy, and seismic/structural behaviour of the buildings. However, carrying out a combined renovation of windows while including insulation outside the face of the walls results in an improvement of the energy performance of the building by more than 300% compared with the individual renovations (RP₁ or RP₂). Similar conclusions resulted for the seismic behaviour.

In the light of the results, this work can conclude that the multiobjective seismic-energetic retrofitting of buildings can lead to synergies, reducing the economic cost of the solutions due to the reduction of installation times, material, and workmanship needs. This can enable the improvement of the seismic/structural behaviour of buildings in case of a future seismic event of up to 240% compared with purely energy-related rehabilitation works.

6. Future Research Work

Despite being able to comparatively assess and to rank the retrofitting solutions, this comparison was carried out based on an improvement/reduction ratio for each aspect analysed (reduction of both the seismic and the energy demand). The authors are aware that more exhaustive analyses are needed to introduce additional variables, such as the economic saving, the expected annual losses, or the environmental impact (from the construction and the use of the building).

Author Contributions: Conceptualization, M.-V.R.-G.-C., J.D.-B., E.R.-S., A.M.-E. and M.-A.C.; methodology, M.-V.R.-G.-C., J.D.-B., A.M.-E. and M.-A.C.; software, M.-V.R.-G.-C., J.D.-B. and E.R.-S.; validation, M.-V.R.-G.-C. and J.D.-B.; formal analysis, M.-V.R.-G.-C., J.D.-B. and E.R.-S.; investigation, M.-V.R.-G.-C. and J.D.-B.; resources, M.-V.R.-G.-C., J.D.-B. and E.R.-S.; data curation, M.-V.R.-G.-C. and J.D.-B.; writing—original draft preparation, M.-V.R.-G.-C. and J.D.-B.; writing—review and editing, M.-V.R.-G.-C., J.D.-B., A.M.-E. and M.-A.C.; visualization, M.-V.R.-G.-C., J.D.-B. and E.R.-S.; supervision, A.M.-E. and M.-A.C.; project administration, A.M.-E.; funding acquisition, A.M.-E. All authors have read and agreed to the published version of the manuscript.

Funding: This work has been funded by the Consejería de Fomento, Infraestructuras y Ordenación del Territorio de la Junta de Andalucía, grant US.20-01, and the VIII-PPI of the University of Seville through the granting of a scholarship. The funding provided by the Instituto Universitario de Arquitectura y Ciencias de la Construcción is also acknowledged.

Institutional Review Board Statement: Not applicable.

Informed Consent Statement: Not applicable.

Data Availability Statement: Not applicable.

Conflicts of Interest: The authors declare no conflict of interest.

References

1. Ibañez Iralde, N.S.; Pascual, J.; Salom, J. Energy Retrofit of Residential Building Clusters. A Literature Review of Crossover Recommended Measures, Policies Instruments and Allocated Funds in Spain. *Energy Build.* **2021**, *252*, 111409. [[CrossRef](#)]
2. Menna, C.; del Vecchio, C.; di Ludovico, M.; Mauro, G.M.; Ascione, F.; Prota, A. Conceptual Design of Integrated Seismic and Energy Retrofit Interventions. *J. Build. Eng.* **2021**, *38*, 102190. [[CrossRef](#)]
3. Bournas, D.A. Concurrent Seismic and Energy Retrofitting of RC and Masonry Building Envelopes Using Inorganic Textile-Based Composites Combined with Insulation Materials: A New Concept. *Compos. Part B Eng.* **2018**, *148*, 166–179. [[CrossRef](#)]
4. Instituto para la Diversificación y Ahorro de la Energía (IDAE). *Proyecto SECH-SPAHOUSEC. Análisis del Consumo Energético del Sector Residencial en España*; Informe Final; Instituto para la Diversificación y Ahorro de la Energía (IDAE): Madrid, Spain, 2011.
5. European Parliament. *The European Green Deal*; European Parliament: Strasbourg, France, 2019.

6. Freddi, F.; Galasso, C.; Cremen, G.; Dall'Asta, A.; di Sarno, L.; Giaralis, A.; Gutiérrez-Urzúa, F.; Málaga-Chuquitaype, C.; Mitoulis, S.A.; Petrone, C.; et al. Innovations in Earthquake Risk Reduction for Resilience: Recent Advances and Challenges. *Int. J. Disaster Risk Reduct.* **2021**, *60*, 102267. [[CrossRef](#)]
7. Requena-García-Cruz, M.V.; Morales-Esteban, A.; Durand-Neyra, P. Optimal Ductility Enhancement of RC Framed Buildings Considering Different Non-Invasive Retrofitting Techniques. *Eng. Struct.* **2021**, *242*, 112572. [[CrossRef](#)]
8. Sorrentino, L.; Cattari, S.; da Porto, F.; Magenes, G.; Penna, A. Seismic Behaviour of Ordinary Masonry Buildings during the 2016 Central Italy Earthquakes. *Bull. Earthq. Eng.* **2019**, *17*, 5583–5607. [[CrossRef](#)]
9. Avila-Haro, J.A.; Gonzalez-Drigo, R.; Vargas-Alzate, Y.F.; Pujades, L.; Barbat, A. Probabilistic Seismic Assessment of a High-Rise URM Building. *J. Build. Eng.* **2022**, *45*, 103344. [[CrossRef](#)]
10. Sarhosis, V.; Giarlelis, C.; Karakostas, C.; Smyrou, E.; Bal, I.E.; Valkaniotis, S.; Ganas, A. Observations from the March 2021 Thessaly Earthquakes: An Earthquake Engineering Perspective for Masonry Structures. *Bull. Earthq. Eng.* **2022**, *20*, 5483–5515. [[CrossRef](#)]
11. Sarhosis, V.; Dais, D.; Smyrou, E.; Bal, I.E.; Drougkas, A. Quantification of Damage Evolution in Masonry Walls Subjected to Induced Seismicity. *Eng. Struct.* **2021**, *243*, 112529. [[CrossRef](#)]
12. Domínguez, S.; Sendra, J.J.; León, A.L.; Esquivias, P.M. Towards Energy Demand Reduction in Social Housing Buildings: Envelope System Optimization Strategies. *Energies* **2012**, *5*, 2263–2287. [[CrossRef](#)]
13. Segovia-Verjel, M.L.; Requena-García-Cruz, M.V.; De-Justo-Moscardó, E.; Morales-Esteban, A. Optimal Seismic Retrofitting Techniques for URM School Buildings Located in the Southwestern Iberian Peninsula. *PLoS ONE* **2019**, *14*, e0223491. [[CrossRef](#)] [[PubMed](#)]
14. Wang, C.; Forth, J.P.; Nikitas, N.; Sarhosis, V. Retrofitting of Masonry Walls by Using a Mortar Joint Technique; Experiments and Numerical Validation. *Eng. Struct.* **2016**, *117*, 58–70. [[CrossRef](#)]
15. Abeling, S.; Dizhur, D.; Ingham, J. An Evaluation of Successfully Seismically Retrofitted URM Buildings in New Zealand and Their Relevance to Australia. *Australian J. Struct. Eng.* **2018**, *19*, 234–244. [[CrossRef](#)]
16. Shabdin, M.; Attari, N.K.A.; Zargarán, M. Experimental Study on Seismic Behavior of Un-Reinforced Masonry (URM) Brick Walls Strengthened with Shotcrete. *Bull. Earthq. Eng.* **2018**, *16*, 3931–3956. [[CrossRef](#)]
17. Spinella, N. Push-over Analysis of a Rubble Full-Scale Masonry Wall Reinforced with Stainless Steel Ribbons. *Bull. Earthq. Eng.* **2018**, *17*, 497–518. [[CrossRef](#)]
18. Garcia-Ramonda, L.; Pelà, L.; Roca, P.; Camata, G. Experimental Cyclic Behaviour of Shear Masonry Walls Reinforced with Single and Double Layered Steel Reinforced Grout. *Constr. Build. Mater.* **2022**, *320*, 126053. [[CrossRef](#)]
19. Proença, J.M.; Gago, A.S.; Vilas Boas, A. Structural Window Frame for In-Plane Seismic Strengthening of Masonry Wall Buildings. *Int. J. Archit. Herit.* **2019**, *13*, 98–113. [[CrossRef](#)]
20. Proença, J.; Gago, A.S.; Cardoso, J.; Córias, V.; Paula, R. Development of an Innovative Seismic Strengthening Technique for Traditional Load-Bearing Masonry Walls. *Bull. Earthq. Eng.* **2012**, *1*, 113–133. [[CrossRef](#)]
21. Turco, V.; Secondin, S.; Morbin, A.; Valluzzi, M.R.; Modena, C. Flexural and Shear Strengthening of Un-Reinforced Masonry with FRP Bars. *Compos. Sci. Technol.* **2006**, *66*, 289–296. [[CrossRef](#)]
22. Broderick, Á.; Byrne, M.; Armstrong, S.; Sheahan, J.; Coggins, A.M. A Pre and Post Evaluation of Indoor Air Quality, Ventilation, and Thermal Comfort in Retrofitted Co-Operative Social Housing. *Build. Environ.* **2017**, *122*, 126–133. [[CrossRef](#)]
23. Recart, C.; Sturts Dossick, C. Hygrothermal Behavior of Post-Retrofit Housing: A Review of the Impacts of the Energy Efficiency Upgrade Strategies. *Energy Build.* **2022**, *262*, 112001. [[CrossRef](#)]
24. Yang, X.; Zhao, L.; Bruse, M.; Meng, Q. An Integrated Simulation Method for Building Energy Performance Assessment in Urban Environments. *Energy Build.* **2012**, *54*, 243–251. [[CrossRef](#)]
25. Ratti, C.; Baker, N.; Steemers, K. Energy Consumption and Urban Texture. *Energy Build.* **2005**, *37*, 762–776. [[CrossRef](#)]
26. Rodrigues, E.; Amaral, A.R.; Gaspar, A.R.; Gomes, Á. An Approach to Urban Quarter Design Using Building Generative Design and Thermal Performance Optimization. *Energy Procedia* **2015**, *78*, 2899–2904. [[CrossRef](#)]
27. Mangan, S.D.; Koclar Oral, G.; Erdemir Kocagil, I.; Sozen, I. The Impact of Urban Form on Building Energy and Cost Efficiency in Temperate-Humid Zones. *J. Build. Eng.* **2021**, *33*, 101626. [[CrossRef](#)]
28. Caprino, A.; Lorenzoni, F.; Carnieletto, L.; Feletto, L.; de Carli, M.; da Porto, F. Integrated Seismic and Energy Retrofit Interventions on a URM Masonry Building: The Case Study of the Former Courthouse in Fabriano. *Sustainability* **2021**, *13*, 9592. [[CrossRef](#)]
29. Shen, Y.; Yarnold, M. A Novel Sensitivity Analysis of Commercial Building Hybrid Energy-Structure Performance. *J. Build. Eng.* **2021**, *43*, 102808. [[CrossRef](#)]
30. Formisano, A.; Vaiano, G.; Fabbrocino, F. Seismic and Energetic Interventions on a Typical South Italy Residential Building: Cost Analysis and Tax Deduction. *Front. Built Environ.* **2019**, *5*, 12. [[CrossRef](#)]
31. Copiello, S.; Donati, E. Is Investing in Energy Efficiency Worth It? Evidence for Substantial Price Premiums but Limited Profitability in the Housing Sector. *Energy Build.* **2021**, *251*, 111371. [[CrossRef](#)]
32. de Angelis, A.; Ascione, F.; de Masi, R.; Pecce, M.; Vanoli, G. A Novel Contribution for Resilient Buildings. Theoretical Fragility Curves: Interaction between Energy and Structural Behavior for Reinforced Concrete Buildings. *Buildings* **2020**, *10*, 194. [[CrossRef](#)]
33. de Angelis, A.; Tariello, F.; de Masi, R.F.; Pecce, M.R. Comparison of Different Solutions for a Seismic and Energy Retrofit of an Auditorium. *Sustainability* **2021**, *13*, 8761. [[CrossRef](#)]

34. Marini, A.; Passoni, C.; Belleri, A.; Feroldi, F.; Preti, M.; Metelli, G.; Riva, P.; Giuriani, E.; Plizzari, G. Combining Seismic Retrofit with Energy Refurbishment for the Sustainable Renovation of RC Buildings: A Proof of Concept. *Eur. J. Environ. Civ. Eng.* **2022**, *26*, 2475–2495. [[CrossRef](#)]
35. Negro, E.; D’Amato, M.; Cardinale, N. Non-Invasive Methods for Energy and Seismic Retrofit in Historical Building in Italy. *Front. Built Environ.* **2019**, *5*, 125. [[CrossRef](#)]
36. Formisano, A.; Vaiano, G. Combined Energy-Seismic Retrofit of Existing Historical Masonry Buildings: The Novel “DUO System” Coating System Applied to a Case Study. *Heritage* **2021**, *4*, 4629–4646. [[CrossRef](#)]
37. D’Angola, A.; Manfredi, V.; Masi, A.; Mecca, M. Energy and Seismic Rehabilitation of RC Buildings through an Integrated Approach: An Application Case Study. In *Green Energy Advances*; IntechOpen: London, UK, 2019. [[CrossRef](#)]
38. Menna, C.; Felicioni, L.; Negro, P.; Lupišek, A.; Romano, E.; Prota, A.; Hájek, P. Review of Methods for the Combined Assessment of Seismic Resilience and Energy Efficiency towards Sustainable Retrofitting of Existing European Buildings. *Sustain. Cities Soc.* **2022**, *77*, 103556. [[CrossRef](#)]
39. Requena-García-Cruz, M.V.; Morales-Esteban, A.; Durand-Neyra, P.; Estêvão, J.M.C. An Index-Based Method for Evaluating Seismic Retrofitting Techniques. Application to a Reinforced Concrete Primary School in Huelva. *PLoS ONE* **2019**, *14*, e0215120. [[CrossRef](#)]
40. Angiolilli, M.; Lagomarsino, S.; Cattari, S.; Degli Abbatì, S. Seismic Fragility Assessment of Existing Masonry Buildings in Aggregate. *Eng. Struct.* **2021**, *247*, 113218. [[CrossRef](#)]
41. Spanish Ministry of Housing MV-201. *Unreinforced Ceramic Masonry Walls [Muros Resistentes de Fábrica de Ladrillo]*; Spanish Ministry of Housing: Madrid, Spain, 1972.
42. de-Miguel-Rodríguez, J.; Morales-Esteban, A.; Requena-García-Cruz, M.-V.; Zapico-Blanco, B.; Segovia-Verjel, M.-L.; Romero-Sánchez, E.; Carvalho-Estêvão, J.M. Fast Seismic Assessment of Built Urban Areas with the Accuracy of Mechanical Methods Using a Feedforward Neural Network. *Sustainability* **2022**, *14*, 5274. [[CrossRef](#)]
43. McKenna, F.; Fenves, G.L.; Scott, M.H. *OpenSees: Open System for Earthquake Engineering Simulation*; Pacific Earthquake Engineering Research Center: Berkeley, CA, USA, 2000.
44. Petracca, M.; Candeloro, F.; Camata, G. *STKO User Manual*; ASDEA Software Technology: Pescara, Italy, 2017.
45. The MathWorks Inc. *MATLAB and Statistics Toolbox Release 2018b*; The MathWorks Inc.: Natick, MA, USA, 2018.
46. D’Altri, A.M.; Sarhosis, V.; Milani, G.; Rots, J.; Cattari, S.; Lagomarsino, S.; Sacco, E.; Tralli, A.; Castellazzi, G.; de Miranda, S. Modeling Strategies for the Computational Analysis of Unreinforced Masonry Structures: Review and Classification. *Arch. Comput. Methods Eng.* **2020**, *27*, 1153–1185. [[CrossRef](#)]
47. Lagomarsino, S.; Penna, A.; Galasco, A.; Cattari, S. TREMURI Program: An Equivalent Frame Model for the Nonlinear Seismic Analysis of Masonry Buildings. *Eng. Struct.* **2013**, *56*, 1787–1799. [[CrossRef](#)]
48. Serena, C.; Magenes, G. Benchmarking the Software Packages to Model and Assess the Seismic Response of Unreinforced Masonry Existing Buildings through Nonlinear Static Analyses. *Bull. Earthq. Eng.* **2021**, *20*, 1901–1936. [[CrossRef](#)]
49. Requena-García-Cruz, M.-V.; Cattari, S.; Bento, R.; Morales-Esteban, A. Comparative Study of Alternative Equivalent Frame Approaches for the Seismic Assessment of Masonry Buildings in OpenSees (Under Review). *J. Build. Eng.* **2022**, *in press*.
50. Raka, E.; Spacone, E.; Sepe, V.; Camata, G. Advanced Frame Element for Seismic Analysis of Masonry Structures: Model Formulation and Validation. *Earthq. Eng. Struct. Dyn.* **2015**, *44*, 2489–2506. [[CrossRef](#)]
51. Beyer, K.; Eeri, M.; Dazio, A. Quasi-Static Cyclic Tests on Masonry Spandrels. *Earthq. Spectra* **2012**, *28*, 907–929. [[CrossRef](#)]
52. Turnšek, V.; Čačovič, F. Some Experimental Results on the Strength of Brick Masonry Walls. In *Proceedings of the Second International Brick Masonry Conference, Stoke-on-Trent, England, UK, 12–15 April 1971*; pp. 149–156.
53. Cattari, S.; Camilletti, D.; Lagomarsino, S.; Bracchi, S.; Rota, M.; Penna, A. Masonry Italian Code-Conforming Buildings. Part 2: Nonlinear Modelling and Time-History Analysis. *J. Earthq. Eng.* **2018**, *22*, 2010–2040. [[CrossRef](#)]
54. Spanish Ministry for the Ecological Transfer [Ministerio para la Transición Ecológica y el Reto Demográfico]. *Processes for the Certification of Buildings*; Spanish Ministry for the Ecological Transfer: Madrid, Spain, 2022.
55. Spanish Ministry of Public Works [Ministerio de Fomento de España]. *Spanish Technical Code of Buildings [Código Técnico de La Edificación (CTE)]*; Spanish Ministry of Public Works: Madrid, Spain, 2006.
56. Spanish Ministry of Transports Mobility and Urban Agenda [Ministerio de Transportes Movilidad y Agenda Urbana]. *Basic Document: Energy Saving [Documento Básico HE-Ahorro de Energía]*; Spanish Ministry of Transports Mobility and Urban Agenda: Madrid, Spain, 2022.
57. de la Flor, F.J.S.; Domínguez, S.Á.; Félix, J.L.M.; Falcón, R.G. Climatic Zoning and Its Application to Spanish Building Energy Performance Regulations. *Energy Build.* **2008**, *40*, 1984–1990. [[CrossRef](#)]
58. Spanish Ministry of Transports Mobility and Urban Agenda [Ministerio de Transportes Movilidad y Agenda Urbana]. *Basic Document: Healthiness [Documento Básico HS-Salubridad]*; Spanish Ministry of Transports Mobility and Urban Agenda: Madrid, Spain, 2022.
59. Instituto para la Diversificación y Ahorro de la Energía (IDAE). *Condiciones de Aceptación de Procedimientos Alternativos a LiDER y CALENER*; Instituto para la Diversificación y Ahorro de la Energía (IDAE): Madrid, Spain, 2009.
60. Spanish Ministry of Public Works [Ministerio de Fomento]. *Atlas de Puentes Térmicos DA DB-HE/3*; Spanish Ministry of Public Works [Ministerio de Fomento]: Madrid, Spain, 2006.

61. Fernández-Agüera, J.; Domínguez-Amarillo, S.; Sendra, J.J.; Suarez, R. Predictive Models for Airtightness in Social Housing in a Mediterranean Region. *Sustain. Cities Soc.* **2019**, *51*, 101695. [[CrossRef](#)]
62. León, Á.L.; Domínguez, S.; Campano, M.A.; Ramírez-Balas, C. Reducing the Energy Demand of Multi-Dwelling Units in a Mediterranean Climate Using Solar Protection Elements. *Energies* **2012**, *5*, 3398–3424. [[CrossRef](#)]
63. Santamaria, J.; Girón, S.; Campano, M.A. Economic Assessments of Passive Thermal Rehabilitations of Dwellings in Mediterranean Climate. *Energy Build.* **2016**, *128*, 772–784. [[CrossRef](#)]
64. Petrovčič, S.; Kilar, V. Design Considerations for Retrofitting of Historic Masonry Structures with Externally Bonded FRP Systems. *Int. J. Archit. Herit.* **2020**, *16*, 957–976. [[CrossRef](#)]
65. Fernández-Agüera, J.; Domínguez-Amarillo, S.; Sendra, J.J.; Suárez, R. An Approach to Modelling Envelope Airtightness in Multi-Family Social Housing in Mediterranean Europe Based on the Situation in Spain. *Energy Build.* **2016**, *128*, 236–253. [[CrossRef](#)]
66. Salehi, A.; Torres, I.; Ramos, A. Experimental Analysis of Building Airtightness in Traditional Residential Portuguese Buildings. *Energy Build.* **2017**, *151*, 198–205. [[CrossRef](#)]
67. Feijó-Muñoz, J.; Pardal, C.; Echarri, V.; Fernández-Agüera, J.; Assiego de Larriva, R.; Montesdeoca Calderín, M.; Poza-Casado, I.; Padilla-Marcos, M.Á.; Meiss, A. Energy Impact of the Air Infiltration in Residential Buildings in the Mediterranean Area of Spain and the Canary Islands. *Energy Build.* **2019**, *188–189*, 226–238. [[CrossRef](#)]